Computers and Concrete, *Vol. 25, No. 3* (*2020*) *225-244*
DOI: https://doi.org/10.12989/cac.2020.25.3.225

Influence of boundary conditions on the bending and free vibration behavior of FGM sandwich plates using a four-unknown refined integral plate theory

Mohammed Cherif Rahmani[1], Abdelhakim Kaci*[1,2], Abdelmoumen Anis Bousahla[3], Fouad Bourada[1,4], Abdeldjebbar Tounsi[1], E.A. Adda Bedia[5], S.R. Mahmoud[6], Kouider Halim Benrahou[1] and Abdelouahed Tounsi[1,5]

[1]*Material and Hydrology Laboratory, Faculty of Technology, Civil Engineering Department, University of Sidi Bel Abbes, Algeria*
[2]*Faculté de Technologie, Département de Génie Civil et Hydraulique, Université Dr Tahar Moulay, BP 138 Cité En-Nasr 20000 Saida, Algérie*
[3]*Laboratoire de Modélisation et Simulation Multi-échelle, Département de Physique, Faculté des Sciences Exactes, Département de Physique, Université de Sidi Bel Abbés, Algeria*
[4]*Département des Sciences et de la Technologie, Centre Universitaire de Tissemsilt, BP 38004 Ben Hamouda, Algérie*
[5]*Department of Civil and Environmental Engineering, King Fahd University of Petroleum & Minerals, 31261 Dhahran, Eastern Province, Saudi Arabia*
[6]*GRC Department, Jeddah Community College, King Abdulaziz University, Jeddah, Saudi Arabia*

(*Received January 6, 2020, Revised February 24, 2020, Accepted February 29, 2020*)

Abstract. The influence of boundary conditions on the bending and free vibration behavior of functionally graded sandwich plates resting on a two-parameter elastic foundation is examined using an original novel high order shear theory. The Hamilton's principle is used herein to derive the equations of motion. The number of unknowns and governing equations of the present theory is reduced, and hence makes it simple to use. This theory includes indeterminate integral variables and contains only four unknowns in which any shear correction factor not used, with even less than the conventional theory of first shear strain (FSDT). Unlike any other theory, the number of unknown functions involved in displacement field is only four, as against five, six or more in the case of other shear deformation theories. Galerkin's approach is utilized for FGM sandwich plates with six different boundary conditions. The accuracy of the proposed solution is checked by comparing it with other closed form solutions available in the literature.

Keywords: sandwich plates; functionally graded materials; new four-unknown refined shear deformation theory and various boundary conditions

1. Introduction

Sandwich structures have a good ratio of stiffness to mass, which is why they are found in many applications. Many studies show that under certain conditions, these structures also have good energy absorption capabilities, making them potential candidates for protection against shock waves or impacts (Goldsmith *et al*. 1997, Radford *et al*. 2006, Katariya *et al*. 2017, 2018, Rajabi and Mohammadimehr 2019, Mehar *et al*. 2019, Mirjavadi *et al*. 2019b, Akbas 2019, Kolahchi *et al*. 2020, Eltaher and Mohamed 2020). These plates are generally fabricated from three layers. The two face sheets adhesively bonded to the core. Since the variations in the rigidity and the material properties of the layers are much more severe in sandwich plates with soft cores in comparison to the traditional composite plates, influence of the transverse shear and normal strains and stresses are more significant in the mentioned sandwich plates.

However, the sudden variation in material characteristics within the interface between different materials can lead to face sheet/core delamination, which is a dangerous problem in sandwich construction. To improve the resistance of sandwich structures to such type of failure, the concept of a functionally graded material (FGM) is being actively applied in plate design. This continuously varying composition eliminates interface problems, and thus, the stress distributions are smooth. FGMs are now developed for general use as structural elements in different applications. An extensive range of plate theories have been developed to analyze the static, vibration, and buckling of advanced functionally graded structures due to the increased relevance of the FGMs structural components in the design of engineering structures (Kolahchi *et al*. 2017b, Hajmohammad *et al*. 2017, Ghorbanpour *et al*. 2016, Benferhat *et al*. 2016, Neves *et al*. 2017, Giunta *et al*. 2016, Kar and Panda 2016 and 2017, Akbaş 2018, Eltaher *et al*. 2018, Faleh *et al*. 2018, Selmi and Bisharat 2018, Hussain *et al*. 2019, Avcar 2019). In general, these plate theories can be divided into three main categories, namely: classical plate theory (CPT), first-order shear deformation plate theory (FSDT) and higher-order plate theory (HSDT). The consequence of the Kirchhoff hypothesis is that the transverse shear strains are zero, and consequently, the transverse stresses do not enter the theory. The theory is known as the Kirchhoff plate theory and it is an extension

*Corresponding author, Professor
E-mail: kaci_abdelhakim@yahoo.fr

ISSN: 1598-8198 (Print), 1598-818X (Online)

of Euler Bernoulli beam theory. Often Kirchhoff plate theory is referred to as the classical plate theory. It does not include shear effects and is therefore applicable to thin plates only (He *et al*. 2017, Woo *et al*. 2006, Abrate 2008, Zhang and Zhou 2008, Arefi 2015, Darilmaz 2015, Pradhan and Chakraverty 2015). The classical plate theory (CPT) will give erroneous results when being used for thick plates, especially plates made of advanced composites (Liu 2011). The first-order shear deformation plate theory (FSDT) is an extension of Kirchhoff plate theory. In this plate theory the basic equations are derived by assumption that the in-plane displacements are linearly distributed across the plate thickness. This leads to the transverse shear stresses being constant across the plate thickness, so the zero shear stress condition on the plate face is not satisfied. This forces the use of shear correction factors, comparable to the need for shear correction factors in the Timoshenko beam theory. Mindlin plate theory is often referred to as first order shear deformation plate theory, and it has been extensively used in the analysis of shear flexible plates and shells. But when Mindlin plate theory is applied to composite plates, the difficulty in accurately evaluating the shear correction factors presents the shortcomings of FSDT (Shi 2007). The FSDT theory allows relatively thick plates to be modelled and their accuracy will depend on the validity of the correction factor used. Thus, to better predict the behaviour of plates, higher order shear deformation theories (HSDTs) were proposed to overcome the drawback of CPT and FSDT. To properly approximate the nonlinear distribution of transverse shear strains along the plate thickness, quite a number of higher order shear deformation plate theories were developed. Such HSDTs have proven to be highly applicable to laminated composite plates. The HSDTs satisfy zero shear stress conditions at top and bottom surfaces of plates. A shear correction factor is, therefore, not required. The high-order using the polynomial shear functions (Reddy 1984, Nguyen *et al*. 2013, Nguyen *et al*. 2017, Nguyen *et al*. 2015), trigonometric functions (Touratier 1991, Thai *et al*. 2014, Nguyen *et al*. 2014) and other theories have been developed to overcome the use of shear correction factor .

In this article, a new and simple plate theory is proposed to study the bending and free vibration of sandwich plate resting on Winkler-Pasternak elastic substrate medium with various boundary conditions. Integral terms are included in the proposed displacement field to reduce the number of unknowns and governing equations. Implementing Hamilton's principle, the equations of motion are obtained and they are solved using Galerkin's method for different boundary conditions. Analytical solutions for bending and vibration four various boundary conditions resting on Winkler-Pasternak elastic foundation are illustrated and the computed results are compared with the available solutions in the literature. Numerical examples are illustrated to check the accuracy of the present formulation in predicting the bending and vibration behaviors and the influences of several parameters are discussed.

2. Theoretical formulation

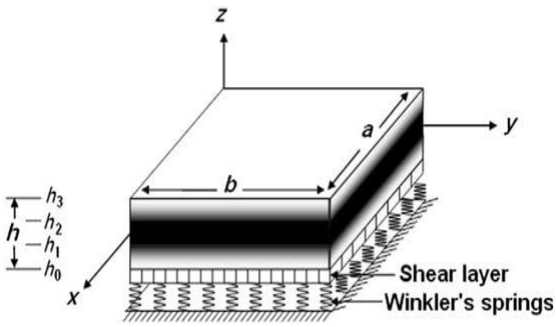

Fig. 1 Geometry of the FGM sandwich plate resting on elastic foundations

2.1 The material properties of FG sandwich plates

Consider a composite structure made of three isotropic layers of arbitrary thickness h, length a and width b . The FGM sandwich plate is supported at four edges defined in the (x, y, z) coordinate system with x- and y-axes located in the middle plane (z=0) and its origin placed at the corner of the plate. The vertical positions of the two interfaces between the core and faces layers are denoted, respectively, by h_1 and h_2. The sandwich core is a ceramic material and skins are composed of a functionally graded material across the thickness direction. The bottom skin varies from a metal-rich surface (z=h_0=−h/2) to a ceramic-rich surface while the top skin face varies from a ceramic-rich surface to a metal-rich surface (z=h_3=h/2). It is assumed to be rested on a Winkler-Pasternak type elastic foundation with the Winkler stiffness of k_w and shear stiffness of k_s as illustrated in Fig. 1.

The material properties of FG face sheets are assumed to vary continuously through the plate thickness by a power law distribution as (Praveen and Reddy 1998, Jha *et al*. 2012, Kar and Panda 2015b, Ramteke *et al*. 2019, Sahouane *et al*. 2019, Zouatnia *et al*. 2019)

$$P(z)=\left(P_c-P_m\right)V^{(n)}+P_m, \quad (n=1,2,3) \tag{1}$$

where P denotes the effective material characteristic such as Young's modulus E, Poisson's ratio ν, and mass density ρ; subscripts c and m indicate the ceramic and metal phases, respectively; and V is the volume fraction of the ceramic phase is obtained from a simple rule of mixtures as

$$\begin{aligned} V^{(1)} &= \left(\frac{z-h_0}{h_1-h_0}\right)^p, && z\in\left[h_0,h_1\right] \\ V^{(2)} &= 1, && z\in\left[h_1,h_2\right] \\ V^{(3)} &= \left(\frac{z-h_3}{h_2-h_3}\right)^p, && z\in\left[h_2,h_3\right] \end{aligned} \tag{2}$$

where $V^{(n)}$, (n=1,2,3), denotes the volume fraction function of layer n; p is the volume fraction index ($0\le p\le+\infty$), which dictates the material variation profile through the thickness. Note that the core of the present sandwich and any isotropic material can be obtained as a particular case of the power-law function by setting p=0. The volume fraction for the metal phase is given as V_m=1−V_c.

2.2 Constitutive equations

For elastic and isotropic FGMs, the constitutive relations can be written as

$$\begin{Bmatrix}\sigma_x\\ \sigma_y\\ \tau_{xy}\end{Bmatrix}^{(n)} = \begin{bmatrix}Q_{11} & Q_{12} & 0\\ Q_{12} & Q_{22} & 0\\ 0 & 0 & Q_{66}\end{bmatrix}^{(n)} \begin{Bmatrix}\varepsilon_x\\ \varepsilon_y\\ \gamma_{xy}\end{Bmatrix}^{(n)}$$
$$\begin{Bmatrix}\tau_{yz}\\ \tau_{xz}\end{Bmatrix}^{(n)} = \begin{bmatrix}Q_{44} & 0\\ 0 & Q_{55}\end{bmatrix}^{(n)} \begin{Bmatrix}\gamma_{yz}\\ \gamma_{xz}\end{Bmatrix}^{(n)} \tag{3}$$

where (σ_x, σ_y, σ_y, τ_{xy}, τ_{yz}, τ_{yx}) and (ε_x, ε_y, γ_{xy}, γ_{yz}, γ_{yx}) are the stress and strain components, respectively. Using the material properties defined in Eq. (1), stiffness coefficients, Q_{ij}, can be expressed as

$$Q_{11}^{(n)} = Q_{22}^{(n)} = \frac{E^{(n)}(z)}{1-\nu^2}, \tag{4a}$$

$$Q_{12}^{(n)} = \frac{\nu\, E^{(n)}(z)}{1-\nu^2}, \tag{4b}$$

$$Q_{44}^{(n)} = Q_{55}^{(n)} = Q_{66}^{(n)} = \frac{E^{(n)}(z)}{2(1+\nu)}, \tag{4c}$$

In this study, further simplifying supposition are made to the conventional HSDT so that the number of unknowns is reduced. The displacement field of the conventional HSDT is given by

$$\begin{aligned} u(x,y,z,t) &= u_0(x,y,t) - z\frac{\partial w_0}{\partial x} + f(z)\phi_x(x,y,t)\\ v(x,y,z,t) &= v_0(x,y,t) - z\frac{\partial w_0}{\partial y} + f(z)\phi_y(x,y,t)\\ w(x,y,z) &= w_0(x,y,t) \end{aligned} \tag{5}$$

u_0, v_0, w_0, ϕ_x, ϕ_y are the five unknown displacement of the mid-plane of the plate. By considering that $\phi_x = k_1\int\theta(x,y,t)\,dx$ and $\phi_y = k_2\int\theta(x,y,t)\,dy$. The displacement fields mentioned above can be written as follows

$$\begin{aligned} u(x,y,z,t) &= u_0(x,y,t) - z\frac{\partial w_0}{\partial x} + k_1\, f(z)\int\theta(x,y,t)dx\\ v(x,y,z,t) &= v_0(x,y,t) - z\frac{\partial w_0}{\partial y} + k_2\, f(z)\int\theta(x,y,t)dy\\ w(x,y,z,t) &= w_0(x,y,t) \end{aligned} \tag{6}$$

The constants k_1 and k_2 depends on the geometry. The shape functions $f(z)$ are chosen to satisfy the stress-free boundary conditions on the top and bottom surfaces of the plate, thus a shear correction factor is not required. In this study, the shape function is considered.

$$f(z) = \frac{(h/\pi)\sinh\left(\frac{\pi}{h}z\right) - z\cosh(\pi/2)}{[\cosh(\pi/2) - 1]} \tag{7}$$

It can be observed that the kinematic in Eq. (6) uses only four unknowns (u_0, v_0, w_0 and θ).

The five nonzero linear strain components compatible with the displacement field in Eq. (6) are

$$\begin{Bmatrix}\varepsilon_x\\ \varepsilon_y\\ \gamma_{xy}\end{Bmatrix} = \begin{Bmatrix}\varepsilon_x^0\\ \varepsilon_y^0\\ \gamma_{xy}^0\end{Bmatrix} + z\begin{Bmatrix}k_x^b\\ k_y^b\\ k_{xy}^b\end{Bmatrix} + f(z)\begin{Bmatrix}k_x^s\\ k_y^s\\ k_{xy}^s\end{Bmatrix},$$
$$\begin{Bmatrix}\gamma_{yz}\\ \gamma_{xz}\end{Bmatrix} = g(z)\begin{Bmatrix}\gamma_{yz}^0\\ \gamma_{xz}^0\end{Bmatrix} \tag{8}$$

where

$$\begin{Bmatrix}\varepsilon_x^0\\ \varepsilon_y^0\\ \gamma_{xy}^0\end{Bmatrix} = \begin{Bmatrix}\dfrac{\partial u_0}{\partial x}\\ \dfrac{\partial v_0}{\partial y}\\ \dfrac{\partial u_0}{\partial y} + \dfrac{\partial v_0}{\partial x}\end{Bmatrix}, \quad \begin{Bmatrix}k_x^b\\ k_y^b\\ k_{xy}^b\end{Bmatrix} = \begin{Bmatrix}-\dfrac{\partial^2 w_0}{\partial x^2}\\ -\dfrac{\partial^2 w_0}{\partial y^2}\\ -2\dfrac{\partial^2 w_0}{\partial x\partial y}\end{Bmatrix},$$
$$\begin{Bmatrix}k_x^s\\ k_y^s\\ k_{xy}^s\end{Bmatrix} = \begin{Bmatrix}k_1\theta\\ k_2\theta\\ k_1\dfrac{\partial}{\partial y}\int\theta\,dx + k_2\dfrac{\partial}{\partial x}\int\theta\,dy\end{Bmatrix}, \quad \begin{Bmatrix}\gamma_{yz}^0\\ \gamma_{xz}^0\end{Bmatrix} = \begin{Bmatrix}k_2\int\theta\,dy\\ k_1\int\theta\,dx\end{Bmatrix} \tag{9}$$

and $g(z)$ is given as follows

$$g(z) = f'(z) \tag{10}$$

The integrals defined in the above equations shall be resolved by a type method and can be written as follows

$$\begin{aligned} &\int\theta\,dx = A'\frac{\partial\theta}{\partial x};\quad \int\theta\,dy = B'\frac{\partial\theta}{\partial y};\\ &k_1A'\frac{\partial\theta(x,y)}{\partial x} = \varphi_x(x,y);\quad k_2B'\frac{\partial\theta(x,y)}{\partial y} = \varphi_y(x,y) \end{aligned} \tag{11}$$

where the coefficients A' and B' are expressed according to the type of solution used, in this case for Exact solutions for sandwich plates for different boundary conditions. Therefore, A', B', k_1 and k_2 are expressed as follows:

2.3 Governing equations

Hamilton's principle is used herein to derive the equations of motion. The principle can be stated in analytical form as (Mehar *et al*. 2015, Kar and Panda 2015c, Kolahchi *et al*. 2016, 2017a, Ebrahimi and Barati 2017a, 2019, Akbas 2017, Eltaher *et al*. 2018, Mouli *et al*.

Table 1 value of A', B', k_1 and k_2 for different boundary conditions

Boundary conditions	A'	k_1	B'	k_2
SSSS	$-1/\lambda^2$	λ^2	$-1/\mu^2$	μ^2
CSCS	$-1/4\lambda^2$	$4\lambda^2$	$-1/\mu^2$	μ^2
CCCC	$-1/4\lambda^2$	$4\lambda^2$	$-1/4\mu^2$	$4\mu^2$
FCFC	$-1/8\lambda^2$	$8\lambda^2$	$-1/4\mu^2$	$4\mu^2$

2018, Safa *et al*. 2019, Hadji *et al*. 2019, Hamed *et al*. 2020, Barati and Shahverdi 2020, Eltaher *et al*. 2020)

$$\int_0^t \delta(U + U_F - V + K)dt = 0, \tag{12}$$

where U, U_F, V and K are, respectively, the strain energy, additional strain energy induced by the elastic foundations, work of external (applied) forces and kinetic energy. The first variation of strain energy can be written as

$$\begin{aligned}\delta U &= \int_A \int_{-h/2}^{h/2} \left(\sigma_x^{(n)}\delta\varepsilon_x + \sigma_y^{(n)}\delta\varepsilon_y + \tau_{xy}^{(n)}\delta\gamma_{xy}\right. \\ &\qquad \left. + \tau_{xz}^{(n)}\delta\gamma_{xz} + \tau_{yz}^{(n)}\delta\gamma_{yz}\right)dAdz \\ &= \int_A \left[N_x\delta\varepsilon_x^0 + N_{xy}\delta\gamma_{xy}^0 + N_y\delta\varepsilon_y^0 + M_x\delta k_x^b\right. \\ &\quad + M_y\delta k_y^b + M_{xy}\delta k_{xy}^b + S_x\delta k_x^s + S_y\delta k_y^s \\ &\quad \left. + S_{xy}\delta k_{xy}^s + Q_{yz}\delta\gamma_{yz}^0 + Q_{xz}\delta\gamma_{xz}^0\right]dA\end{aligned} \tag{13}$$

where A is the top surface.

The stress and moment resultants of the FGM sandwich plate can be obtained by integrating Eq. (3) over the thickness, and are written as

$$\begin{Bmatrix} N_x, & N_y, & N_{xy} \\ M_x, & M_y, & M_{xy} \\ S_x, & S_y, & S_{xy} \end{Bmatrix} = \sum_{n=1}^{3}\int_{h_{n-1}}^{h_n} \left(\sigma_x, \sigma_y, \tau_{xy}\right)^{(n)} \begin{Bmatrix} 1 \\ z \\ f(z) \end{Bmatrix} dz, \tag{14a}$$

$$\left(Q_{xz}, Q_{yz}\right) = \sum_{n=1}^{3}\int_{h_{n-1}}^{h_n} \left(\tau_{xz}, \tau_{yz}\right)^{(n)} g(z)dz. \tag{14b}$$

where h_n and h_{n-1} are the top and bottom z-coordinates of the nth layer.

The strain energy induced by elastic foundations can be defined as

$$\delta U_F = \int_A p\delta w_0 dA \tag{15}$$

where A is the area of top surface and f_e is the density of reaction force of foundation. For the Pasternak foundation model f_e is given by

$$f_e = k_w w_0 - k_{sx}\frac{\partial^2 w_0}{\partial x^2} - k_{sy}\frac{\partial^2 w_0}{\partial y^2} \tag{16}$$

where k_w is the modulus of subgrade reaction (elastic coefficient of the foundation) and k_{sx} and k_{sy} are the shear moduli of the subgrade (shear layer foundation stiffness). If foundation is homogeneous and isotropic, we will get k_{sx}= k_{sy}=k_s. If the shear layer foundation stiffness is neglected, Pasternak foundation becomes a Winkler foundation.

The variation of work done by transverse load q can be expressed as

$$\delta V = -\int_A q\delta w_0 dA \tag{17}$$

The variation of kinetic energy is expressed as

$$\begin{aligned}\delta K &= \int_V \left[\dot{u}\,\delta\dot{u} + \dot{v}\,\delta\dot{v} + \dot{w}\,\delta\dot{w}\right]\rho(z)\,dV \\ &= \int_A \{I_0\left[\dot{u}_0\delta\dot{u}_0 + \dot{v}_0\delta\dot{v}_0 + \dot{w}_0\delta\dot{w}_0\right] \\ &\quad - I_1\left(\dot{u}_0\frac{\partial\delta\dot{w}_0}{\partial x} + \frac{\partial\dot{w}_0}{\partial x}\delta\dot{u}_0 + \dot{v}_0\frac{\partial\delta\dot{w}_0}{\partial y} + \frac{\partial\dot{w}_0}{\partial y}\delta\dot{v}_0\right) \\ &\quad + J_1\left(\left(k_1 A'\right)\left(\dot{u}_0\frac{\partial\delta\dot{\theta}}{\partial x} + \frac{\partial\dot{\theta}}{\partial x}\delta\dot{u}_0\right)\right. \\ &\qquad \left. + \left(k_2 B'\right)\left(\dot{v}_0\frac{\partial\delta\dot{\theta}}{\partial y} + \frac{\partial\dot{\theta}}{\partial y}\delta\dot{v}_0\right)\right) \\ &\quad + I_2\left(\frac{\partial\dot{w}_0}{\partial x}\frac{\partial\delta\dot{w}_0}{\partial x} + \frac{\partial\dot{w}_0}{\partial y}\frac{\partial\delta\dot{w}_0}{\partial y}\right) \\ &\quad + K_2\left(\left(k_1 A'\right)^2\left(\frac{\partial\dot{\theta}}{\partial x}\frac{\partial\delta\dot{\theta}}{\partial x}\right) + \left(k_2 B'\right)^2\left(\frac{\partial\dot{\theta}}{\partial y}\frac{\partial\delta\dot{\theta}}{\partial y}\right)\right) \\ &\quad - J_2\left(\left(k_1 A'\right)\left(\frac{\partial\dot{w}_0}{\partial x}\frac{\partial\delta\dot{\theta}}{\partial x} + \frac{\partial\dot{\theta}}{\partial x}\frac{\partial\delta\dot{w}_0}{\partial x}\right)\right. \\ &\quad \left. + \left(k_2 B'\right)\left(\frac{\partial\dot{w}_0}{\partial y}\frac{\partial\delta\dot{\theta}}{\partial y} + \frac{\partial\dot{\theta}}{\partial y}\frac{\partial\delta\dot{w}_0}{\partial y}\right)\right)\}dA\end{aligned} \tag{18}$$

where dot-superscript convention indicates the differentiation with respect to the time variable t; $\rho(z)$ is the mass density; and $(I_0, I_1, I_2, J_1, J_2, K_2)$ are mass inertias defined as

$$\left(I_0, I_1, I_2\right) = \int_{-h/2}^{h/2}\left(1, z, z^2\right)\rho(z)dz \tag{19a}$$

$$\left(J_1, J_2, K_2\right) = \int_{-h/2}^{h/2}\left(f(z), z\,f(z), f^2(z)\right)\rho(z)dz \tag{19b}$$

Substituting Eqs. (13), (15),(17) and (18) into Eq. (12) and integrating by parts and collecting the coefficients of δu_0, δv_0, δw_0 and $\delta\theta$, the following equations of motion of the plate are obtained as

$$\delta u_0 : \frac{\partial N_x}{\partial x} + \frac{\partial N_{xy}}{\partial y} = I_0\ddot{u}_0 - I_1\frac{\partial\ddot{w}_0}{\partial x} + k_1 A' J_1\frac{\partial\ddot{\theta}}{\partial x}$$

$$\delta v_0 : \frac{\partial N_{xy}}{\partial x} + \frac{\partial N_y}{\partial y} = I_0\ddot{v}_0 - I_1\frac{\partial\ddot{w}_0}{\partial y} + k_2 B' J_1\frac{\partial\ddot{\theta}}{\partial y}$$

$$\begin{aligned}\delta w_0 : \frac{\partial^2 M_x}{\partial x^2} + 2\frac{\partial^2 M_{xy}}{\partial x\partial y} + \frac{\partial^2 M_y}{\partial y^2} + q - f_e \\ = I_0\ddot{w}_0 + I_1\left(\frac{\partial\ddot{u}_0}{\partial x} + \frac{\partial\ddot{v}_0}{\partial y}\right) - I_2\nabla^2\ddot{w}_0 \\ + J_2\left(k_1 A'\frac{\partial^2\ddot{\theta}}{\partial x^2} + k_2 B'\frac{\partial^2\ddot{\theta}}{\partial y^2}\right)\end{aligned}$$

$$\begin{aligned}\delta\theta : -k_1 S_x - k_2 S_y - \left(k_1 A' + k_2 B'\right)\frac{\partial^2 S_{xy}}{\partial x\partial y} \\ + k_1 A'\frac{\partial Q_{xz}}{\partial x} + k_2 B'\frac{\partial Q_{yz}}{\partial y} =\end{aligned}$$

$$
\begin{aligned}
&-J_1\left(k_1 A'\frac{\partial\ddot{u}_0}{\partial x}+k_2 B'\frac{\partial\ddot{v}_0}{\partial y}\right)\\
&-K_2\left(\left(k_1 A'\right)^2\frac{\partial^2\ddot{\theta}}{\partial x^2}+\left(k_2 B'\right)^2\frac{\partial^2\ddot{\theta}}{\partial y^2}\right)\\
&+J_2\left(k_1 A'\frac{\partial^2\ddot{w}_0}{\partial x^2}+k_2 B'\frac{\partial^2\ddot{w}_0}{\partial y^2}\right)
\end{aligned}
\tag{20}
$$

Using Eq. (3) in Eq. (14), the stress resultants of a sandwich plate made up of three layers can be related to the total strains by

$$
\begin{Bmatrix} N\\ M\\ S\end{Bmatrix}=\begin{bmatrix} A & B & B^s\\ B & D & D^s\\ B^s & D^s & H^s\end{bmatrix}\begin{Bmatrix}\varepsilon\\ k^b\\ k^s\end{Bmatrix},\quad Q=A^s\gamma^0 \tag{21}
$$

where

$$
N=\left\{N_x,N_y,N_{xy}\right\}^t,\ M=\left\{M_x,M_y,M_{xy}\right\}^t,\ S=\left\{S_x,S_y,S_{xy}\right\}^t \tag{22a}
$$

$$
\varepsilon=\left\{\varepsilon_x^0,\varepsilon_y^0,\gamma_{xy}^0\right\}^t,\ k^b=\left\{k_x^b,k_y^b,k_{xy}^b\right\}^t,\ k^s=\left\{k_x^s,k_y^s,k_{xy}^s\right\}^t \tag{22b}
$$

$$
A=\begin{bmatrix} A_{11} & A_{12} & 0\\ A_{12} & A_{22} & 0\\ 0 & 0 & A_{66}\end{bmatrix},\ B=\begin{bmatrix} B_{11} & B_{12} & 0\\ B_{12} & B_{22} & 0\\ 0 & 0 & B_{66}\end{bmatrix},\ D=\begin{bmatrix} D_{11} & D_{12} & 0\\ D_{12} & D_{22} & 0\\ 0 & 0 & D_{66}\end{bmatrix} \tag{22c}
$$

$$
B^s=\begin{bmatrix} B_{11}^s & B_{12}^s & 0\\ B_{12}^s & B_{22}^s & 0\\ 0 & 0 & B_{66}^s\end{bmatrix},\ D^s=\begin{bmatrix} D_{11}^s & D_{12}^s & 0\\ D_{12}^s & D_{22}^s & 0\\ 0 & 0 & D_{66}^s\end{bmatrix},\ H^s=\begin{bmatrix} H_{11}^s & H_{12}^s & 0\\ H_{12}^s & H_{22}^s & 0\\ 0 & 0 & H_{66}^s\end{bmatrix} \tag{22d}
$$

$$
Q=\left\{Q_{yz},Q_{xz}\right\}^t,\ \gamma^0=\left\{\gamma_{yz}^0,\gamma_{xz}^0\right\}^t,\ A^s=\begin{bmatrix} A_{44}^s & 0\\ 0 & A_{55}^s\end{bmatrix} \tag{22e}
$$

where A_{ij}, B_{ij}, etc., are the plate stiffness, defined by

$$
\begin{Bmatrix} A_{11} & B_{11} & D_{11} & B_{11}^s & D_{11}^s & H_{11}^s\\ A_{12} & B_{12} & D_{12} & B_{12}^s & D_{12}^s & H_{12}^s\\ A_{66} & B_{66} & D_{66} & B_{66}^s & D_{66}^s & H_{66}^s\end{Bmatrix}=\sum_{n=1}^{3}\int_{h_{n-1}}^{h_n} Q_{11}^{(n)}\left(1,z,z^2,f(z),z\,f(z),f^2(z)\right)\begin{Bmatrix}1\\ \nu^{(n)}\\ \frac{1-\nu^{(n)}}{2}\end{Bmatrix}dz \tag{23a}
$$

and

$$
\left(A_{22},B_{22},D_{22},B_{22}^s,D_{22}^s,H_{22}^s\right)=\left(A_{11},B_{11},D_{11},B_{11}^s,D_{11}^s,H_{11}^s\right),
$$

$$
Q_{11}^{(n)}=\frac{E(z)}{1-\nu^2} \tag{23b}
$$

$$
A_{44}^s=A_{55}^s=\sum_{n=1}^{3}\int_{h_{n-1}}^{h_n}\frac{E(z)}{2(1+\nu)}\left[g(z)\right]^2dz, \tag{23c}
$$

2.4 Equations of motion in terms of displacements

By substituting Eqs. (8) and (21) into Eq. (20), the equilibrium equations can be expressed in terms of displacements (u_0, v_0, w_0 and θ) as

$$
\begin{aligned}
&\delta u_0: L_1u_0+A_{11}L_2v_0-L_3d_1w_0+L_4d_1\theta=0\\
&\delta v_0: A_{11}L_2u_0+L_5v_0-L_3d_2w_0+L_6d_2\theta=0\\
&\delta w_0: L_3\left(d_1u_0+d_2v_0\right)-L_7w_0+L_8\theta=0\\
&\delta\theta: -L_4d_1u_0-L_6d_2v_0+L_8w_0-L_9\theta=0
\end{aligned}
\tag{24}
$$

where the operator L_i are given by

$$
L_1=A_{11}\nabla_x^2-I_0\frac{\partial^2}{\partial t^2},\ L_2=\left(\nu+\bar{\nu}\right)d_{12},\ L_3=B_{11}\nabla^2-I_1\frac{\partial^2}{\partial t^2} \tag{25a}
$$

$$
L_4=B_{11}^s\left[k_1+k_2\nu+\bar{\nu}\left(k_1A'+k_2B'\right)d_{22}\right]-k_1A'J_1\frac{\partial^2}{\partial t^2},\ L_5=A_{11}\nabla_y^2-I_0\frac{\partial^2}{\partial t^2} \tag{25b}
$$

$$
L_6=B_{11}^s\left[k_1\nu+k_2+\bar{\nu}\left(k_1A'+k_2B'\right)d_{11}\right]-k_2B'J_1\frac{\partial^2}{\partial t^2} \tag{25c}
$$

$$
L_7=D_{11}\nabla^4+\left(I_0-I_2\nabla^2\right)\frac{\partial^2}{\partial t^2}+\left(k_w-k_s\nabla^2\right) \tag{25d}
$$

$$
\begin{aligned}
L_8=&D_{11}^s\left[\left(k_1+k_2\nu\right)d_{11}+2\bar{\nu}\left(k_1A'+k_2B'\right)d_{1122}\right.\\
&\left.+\left(k_1\nu+k_2\right)d_{22}\right]-J_2\frac{\partial^2}{\partial t^2}\left(k_1A'd_{11}+k_2B'd_{22}\right)
\end{aligned}
\tag{25e}
$$

$$
\begin{aligned}
L_9=&H_{11}^s\left(k_1^2+2\nu k_1k_2+k_2^2\right)+\bar{\nu}H_{11}^s\left(k_1A'+k_2B'\right)^2d_{1122}\\
&-k_1^2A'^2A_{55}^sd_{11}-k_2^2B'^2A_{55}^sd_{22}\\
&-K_2\frac{\partial^2}{\partial t^2}\left[\left(k_1A'\right)^2d_{11}+\left(k_2B'\right)^2d_{22}\right]
\end{aligned}
\tag{25f}
$$

where d_{ij}, d_{ijl} and d_{ijlm} are the following differential operators:

$$
d_{ij}=\frac{\partial^2}{\partial x_i\partial x_j},\ d_{ijl}=\frac{\partial^3}{\partial x_i\partial x_j\partial x_l},\ d_{ijlm}=\frac{\partial^4}{\partial x_i\partial x_j\partial x_l\partial x_m},\ d_i=\frac{\partial}{\partial x_i},\ (i,j,l,m=1,2). \tag{26a}
$$

and

$$\nabla_x^2 = \frac{\partial^2}{\partial x^2} + \bar{\nu}\frac{\partial^2}{\partial y^2},\quad \nabla_y^2 = \bar{\nu}\frac{\partial^2}{\partial x^2} + \frac{\partial^2}{\partial y^2},$$
$$\nabla^2 = \frac{\partial^2}{\partial x^2} + \frac{\partial^2}{\partial y^2},\quad \nabla^4 = \nabla^2\left(\nabla^2\right),\quad \bar{\nu} = \frac{1-\nu}{2} \tag{26b}$$

3. Exact solutions for FGMs sandwich plates

The exact solution of Eq. (24) for the graded sandwich plate with simply supported (S), clamped (C) or free (F) edges is presented. These boundary conditions are defined as follow:

Simply supported (S)

$$v_0 = w_0 = \frac{\partial\theta}{\partial y} = N_{xx} = M_{xx} = S_{xx} = 0 \qquad at \qquad x = 0, a,$$
$$u_0 = w_0 = \frac{\partial\theta}{\partial x} = N_{yy} = M_{yy} = S_{yy} = 0 \qquad at \qquad y = 0, b. \tag{27}$$

Clamped (C):

$$u_0 = v_0 = w_0 = \frac{\partial\theta}{\partial x} = \frac{\partial\theta}{\partial y} = 0 \qquad at \qquad x = 0, a; \qquad y = 0, b. \tag{28}$$

Free (F):

$$M_{xx} = M_{xy} = Q_{xz} = 0 \qquad at \qquad x = 0, a,$$
$$M_{yy} = M_{xy} = Q_{yz} = 0 \qquad at \qquad y = 0, b. \tag{29}$$

The following representation for the displacement quantities, that satisfy the above boundary conditions, is appropriate in the case of our problem

$$\begin{Bmatrix} u_0 \\ v_0 \\ w_0 \\ \theta \end{Bmatrix} = \sum_{m=1}^{\infty}\sum_{n=1}^{\infty} \begin{Bmatrix} U_{mn}\dfrac{\partial X_m(x)}{\partial x} Y_n(y) e^{i\omega t} \\ V_{mn}\, X_m(x)\dfrac{\partial Y_n(y)}{\partial y} e^{i\omega t} \\ W_{mn} X_m(x) Y_n(y) e^{i\omega t} \\ Z_{mn}\dfrac{\partial^2 X_m(x)}{\partial x^2} Y_n(y) e^{i\omega t} \end{Bmatrix} \tag{30}$$

where $i = \sqrt{-1}$, U_{mn}, V_{mn}, W_{mn} and Z_{mn} are coefficients, and ω is the natural frequency. The functions $X_m(x)$ and $Y_m(y)$ given in Table 2 noting that $\lambda = m\pi/a$, $\mu = n\pi/b$ to satisfy various boundary conditions in Eqs. (27)-(29). The plate is subjected to transverse load q.

The transverse load q is also expanded in the double-Fourier sine series as (Reddy *et al*. 2001)

$$q(x,y) = \sum_{m=1}^{\infty}\sum_{n=1}^{\infty} Q_{mn}\sin(\lambda x)\sin(\mu y) \tag{31}$$

The coefficients Q_{mn} for the case of uniformly distributed load (*UDL*) are defined as follows

$$Q_{mn} = \frac{16 q_0 ab}{\lambda\,\mu}, \quad (m, n = 1,3,5,.....) \tag{32}$$

where q_0 represents the intensity of the load at the plate center.

For the case of a sinusoidally distributed load (SDL), we have

$$m = n = 1 \quad \text{and} \quad Q_{11} = q_0 \tag{33}$$

Substituting expressions (30) into the governing Eqs. (24) and multiplying each equation by the corresponding eigen function then integrating over the domain of solution, we can obtain, after some mathematical manipulations, the following equations

$$\left(\begin{bmatrix} S_{11} & S_{12} & S_{13} & S_{14} \\ S_{21} & S_{22} & S_{23} & S_{24} \\ S_{31} & S_{32} & S_{33} & S_{34} \\ S_{41} & S_{42} & S_{43} & S_{44} \end{bmatrix} - \omega^2 \begin{bmatrix} M_{11} & 0 & M_{13} & M_{14} \\ 0 & M_{22} & M_{23} & M_{24} \\ M_{13} & M_{23} & M_{33} & M_{34} \\ M_{14} & M_{24} & M_{34} & M_{44} \end{bmatrix} \right) \begin{Bmatrix} U_{mn} \\ V_{mn} \\ W_{mn} \\ Z_{mn} \end{Bmatrix} = \begin{Bmatrix} 0 \\ 0 \\ f_q \\ 0 \end{Bmatrix} \tag{34}$$

in which

$$\begin{aligned}
S_{11} &= A_{11}\left(e_{12} + \bar{\nu}\, e_8\right) \\
S_{12} &= A_{11}\left(\nu + \bar{\nu}\right) e_8 \\
S_{13} &= -B_{11}\left(e_8 + e_{12}\right) \\
S_{14} &= B_{11}^s\left[(k_1 + k_2\nu) e_{12} + \bar{\nu}(k_1 A' + k_2 B') e_{20}\right] \\
S_{21} &= A_{11}\left(\nu + \bar{\nu}\right) e_{10} \\
S_{22} &= A_{11}\left(\bar{\nu} e_{10} + e_4\right) \\
S_{23} &= -B_{11}\left(e_{10} + e_4\right) \\
S_{24} &= B_{11}^s\left[(k_1\nu + k_2) e_{10} + \bar{\nu}\left(k_1 A' + k_2 B'\right) e_{21}\right] \\
S_{31} &= -B_{11}\left(e_{13} + e_{11}\right) \\
S_{32} &= -B_{11}\left(e_{11} + e_5\right) \\
S_{33} &= D_{11}\left(e_{13} + e_5 + 2e_{11}\right) + \left(\overline{N}_{xx} - k_{sx}\right) e_9 \\
&\quad + \left(\overline{N}_{yy} - k_{sy}\right) e_3 + k_w e_1 + 2\overline{N}_{xy} e_7 \\
S_{34} &= -D_{11}^s\left[(k_1 + k_2\nu) e_{13} + 2\bar{\nu}\left(k_1 A' + k_2 B'\right) e_{14} + \left(k_1\nu + k_2\right) e_{11}\right] \\
S_{41} &= B_{11}^s\left[(k_1 + k_2\nu) e_{15} + \bar{\nu}\left(k_1 A' + k_2 B'\right) e_{16}\right] \\
S_{42} &= B_{11}^s\left[(k_1\nu + k_2) e_{17} + \bar{\nu}\left(k_1 A' + k_2 B'\right) e_{16}\right] \\
S_{43} &= -D_{11}^s\left[(k_1 + k_2\nu) e_{15} + 2\bar{\nu}\left(k_1 A' + k_2 B'\right) e_{16} + \left(k_1\nu + k_2\right) e_{17}\right] \\
S_{44} &= H_{11}^s\left(k_1^2 + 2\nu k_1 k_2 + k_2^2\right) e_{15} + \bar{\nu} H_{11}^s\left(k_1 A' + k_2 B'\right)^2 e_{18} \\
&\quad - A_{55}^s\left[\left(k_1 A'\right)^2 e_{19} + \left(k_2 B'\right)^2 e_{16}\right]
\end{aligned} \tag{35}$$

and

$$\begin{aligned}
M_{11} &= -I_0 e_6 \\
M_{12} &= 0 \\
M_{13} &= I_1 e_6 \\
M_{14} &= I_1 e_{12} \\
M_{22} &= -I_0 e_2 \\
M_{23} &= I_1 e_2 \\
M_{24} &= J_1 k_2 B' e_{10} \\
M_{31} &= I_1 e_9 \\
M_{32} &= I_1 e_3 \\
M_{33} &= I_0 e_1 - I_2\left(e_9 + e_3\right) \\
M_{34} &= J_2\left(k_2 B' e_{11} + k_1 A' e_{13}\right) \\
M_{41} &= -J_1 k_1 A' e_{15} \\
M_{42} &= -J_1 k_2 B' e_{17} \\
M_{43} &= J_2\left(k_1 A' e_{15} + k_2 B' e_{17}\right) \\
M_{44} &= -J_3\left[\left(k_1 A'\right)^2 e_{19} + \left(k_2 B'\right)^2 e_{16}\right]
\end{aligned} \tag{36}$$

Table 2 The admissible functions $X_m(x)$ and $Y_m(y)$

Boundary conditions			The functions $X_m(x)$ and $Y_m(y)$	
SSSS	$X_m(0)=X_m''(0)=0$ $X_m(a)=X_m''(a)=0$	$Y_n(0)=Y_n''(0)=0$ $Y_n(b)=Y_n''(b)=0$	$sin(\lambda x)$	$sin(\mu y)$
CSCS	$X_m(0)=X_m'(0)=0$ $X_m(a)=X_m''(a)=0$	$Y_n(0)=Y_n'(0)=0$ $Y_n(b)=Y_n''(b)=0$	$sin^2(\lambda x)$	$sin(\mu y)$
CCCC	$X_m(0)=X_m'(0)=0$ $X_m(a)=X_m'(a)=0$	$Y_n(0)=Y_n'(0)=0$ $Y_n(b)=Y_n'(b)=0$	$sin^2(\lambda x)$	$sin^2(\mu y)$
FCFC	$X_m''(0)=X_m'''(0)=0$ $X_m''(a)=X_m'''(a)=0$	$Y_n(0)=Y_n'(0)=0$ $Y_n(b)=Y_n'(b)=0$	$cos^2(\lambda x)[sin^2(\lambda x)+1]$	$sin^2(\mu y)$

- ( )' denotes the derivative with respect to the corresponding coordinates.

Table 3 Material properties used in the FG sandwich plate

Properties	Metal	Ceramic
	Al	Al_2O_3
E (GPa)	70	380
v	0.3	0.3
ρ (kg/m^3)	2707	3800

With

$$(e_6,e_{20},e_8,e_{12})=\int_0^b\int_0^a\left(X_m'Y_n,X_m'''Y_n'',X_m'Y_n'',X_m'''Y_n\right)X_m'Y_n\,dxdy$$

$$(e_2,e_{21},e_4,e_{10})=\int_0^b\int_0^a\left(X_mY_n',X_m'''Y_n',X_mY_n''',X_m''Y_n'\right)X_mY_n'dxdy$$

$$(e_1,e_3,e_5,e_{14})=\int_0^b\int_0^a\left(X_mY_n,X_mY_n'',X_mY_n'''',X_m''''Y_n''\right)X_mY_n\,dxdy$$

$$(e_7,e_9,e_{11},e_{13})=\int_0^b\int_0^a\left(X_m'Y_n',X_m''Y_n,X_m''Y_n'',X_m''''Y_n\right)X_mY_n\,dxdy \quad (37)$$

$$(e_{15},e_{16},e_{17})=\int_0^b\int_0^a\left(X_m''Y_n,X_m''Y_n'',X_mY_n''\right)X_m''Y_n\,dxdy$$

$$(e_{18},e_{19})=\int_0^b\int_0^a\left(X_m''''Y_n'',X_m''''Y_n\right)X_m''Y_n\,dxdy$$

$$f_q=\int_0^b\int_0^a Q_{mn}\sin(\lambda x)\sin(\mu y)\sin(\lambda x)\sin(\mu y)dxdy$$

The non-trivial solution is obtained when the determinant of Eq. (34) equals zero. For the free vibration problem, we have f_q=0. While for the bending analysis, we put ω=0.

4. Numerical results and discussions

In this section, numerical results for bending and free vibration responses are presented for FGM sandwich plates resting on two-parameter elastic foundations with various cases of the boundary conditions. To verify the accuracy of present solution, obtained results are compared with the some existing results in the literature. Material properties of metal and ceramic are chosen as given Table 3.

In the following, we note that several kinds of sandwich plates are used:

- The (1-0-1) FG sandwich plate: The plate is symmetric and made of only two equal-thickness FG layers, i.e., there is no core layer. Thus, we have, h_1=h_2=0
- The (1-1-1) FG sandwich plate: Here, the plate is symmetric and made of three equal-thickness layers. In this case, we have, h_1=−h/6, h_2=h/6
- The (1-2-1) FG sandwich plate: The plate is symmetric and we have: h_1=−h/4, h_2=h/4
- The (1-3-1) FG sandwich plate: The plate is symmetric and we have: h_1=−3h/10, h_2=3h/10
- The (2-1-2) FG sandwich plate, we have: h_1=−h/10, h_2=h/10.
- The (2-2-1) FG sandwich plate: The plate is non-symmetric and we have: h_1=−h/10, h_2=3h/10

For convenience, the following normalization is used in the comparison of all the numerical results

$$w^*=\frac{100D}{q_0a^4}w\left(\frac{a}{2},\frac{b}{2}\right),\qquad \hat{w}=\frac{10E_0h}{q_0a^2}w\left(\frac{a}{2},\frac{b}{2}\right),$$

$$\bar{w}=\frac{10E_ch^3}{q_0a^4}w\left(\frac{a}{2},\frac{b}{2}\right),\qquad \bar{\sigma}_x=\frac{10h^2}{q_0a^2}\sigma_x\left(\frac{a}{2},\frac{b}{2},\frac{h}{2}\right),$$

$$\bar{\tau}_{xz}=\frac{h}{q_0a}\tau_{xz}\left(0,\frac{b}{2},0\right),\quad \omega^*=\omega\frac{a^2}{h},\qquad K_w=\frac{k_wa^4}{D},$$

$$K_s=\frac{k_sa^2}{D},\qquad D=\frac{E_ch^3}{12(1-\nu^2)}$$

where the reference value is taken as E_0=1 GPa

Bending analysis

Table 4 Maximum deflection w^* of simply supported square and rectangular homogeneous plates under uniform loads

Method	a=b			a=0.5b		
	a/h=25	10	5	a/h=25	10	5
Reddy *et al*. (2001)	0.410	0.427	0.490	1.018	1.045	1.043
Cooke and Levinson (1983)	0.410	0.427	0.490	1.018	1.045	1.043
Lee *et al*. (2002)	0.410	0.427	0.490	1.018	1.045	1.043
Present	0.4010	0.427	0.490	1.018	1.045	1.143

Table 5 Nondimensional deflections $10w^*$ of simply supported homogeneous plates resting on elastic foundations and subjected to uniformly distributed loads

a/b	a/h	(10,10)		(10,100)		(100,10)		(100,100)	
		Present	Ref (a)	Present	Ref (a)	Present	Ref (a)	Present	Ref (a)
0.5	5	5.5718	5.5720	1.0371	1.0371	4.0769	4.0769	0.9679	0.9679
	10	5.3562	5.3563	1.0330	1.0330	3.9791	3.9791	0.9649	0.9649
	100	5.2811	5.2811	1.0320	1.0320	3.9446	3.9446	0.9642	0.9642
1.0	5	2.9270	2.9271	0.6451	0.6450	2.4787	2.4788	0.6190	0.6190
	10	2.7059	2.7059	0.6383	0.6383	2.3271	2.3271	0.6132	0.6132
	100	2.6276	2.6276	0.6364	0.6364	2.2724	2.2724	0.6117	0.6117
2.0	5	0.7165	0.7165	0.2207	0.2207	0.6844	0.6844	0.2174	0.2174
	10	0.5736	0.5736	0.2069	0.2069	0.5536	0.5536	0.2041	0.2041
	100	0.5219	0.5219	0.2012	0.2012	0.5056	0.5056	0.1987	0.1987

(a) Zenkour and Radwan (2018)

Table 6 Nondimensional deflection $\widehat{w}$, normal $\bar{\sigma}_x$ and shear stress $\bar{\tau}_{xz}$ of simply supported functionally graded square sandwich plates Subjected to a Sinusoidal Load (a/h=10)

	p	Method	$\widehat{w}$	$\bar{\sigma}_x$	$\bar{\tau}_{xz}$
1-0-1	0	RSDT1 Ref(b)	0.07790303811	1.995500426	0.2461800786
		RSDT2 Ref(b)	0.07790968813	1.994322048	0.2385722368
		Present	0.07790626337	1.993313666	0.2321588570
	1	RSDT1 Ref(b)	0.1960374616	0.9440725801	0.3410283239
		RSDT2 Ref(b)	0.1960877843	0.9436998270	0.3343263458
		Present	0.1961196994	0.9433786862	0.3285935696
	2	RSDT1 Ref(b)	0.2847866148	1.377021358	0.4142621883
		RSDT2 Ref(b)	0.2849023821	1.376618511	0.4091869511
		Present	0.2849875541	1.376265910	0.4046867384
	3	RSDT1 Ref(b)	0.33606390476	1.625907776	0.4750163773
		RSDT2 Ref(b)	0.3362423053	1.625518635	0.4713253791
		Present	0.3363779004	1.625171832	0.4678317078
	4	RSDT1 Ref(b)	0.3645156376	1.762667930	0.5282678443
		RSDT2 Ref(b)	0.3647438193	1.762667930	0.5254079891
		Present	0.3649187246	1.761953313	0.5224579040
	5	RSDT1 Ref(b)	0.3554038421	1.840255874	0.5759064640
		RSDT2 Ref(b)	0.3808987521	1.839886083	0.5733659296
		Present	0.3813670328	1.839547044	0.5705423593
1-1-1	0	RSDT1 Ref(b)	0.07790303811	1.995500426	0.2461800786
		RSDT2 Ref(b)	0.07790968813	1.995500426	0.2385722368
		Present	0.07790626337	1.993313666	0.2321588570
	1	RSDT1 Ref(b)	0.1567130768	0.7538738155	0.2846232298
		RSDT2 Ref(b)	0.1567290438	0.7535245180	0.2777698981
		Present	0.1567348574	0.7532278467	0.2720344806
	2	RSDT1 Ref(b)	0.2106743313	1.018781385	0.3048004591
		RSDT2 Ref(b)	0.2107090884	1.018389504	0.2989262010
		Present	0.2107314888	1.018056327	0.2940124336
	3	RSDT1 Ref(b)	0.2451013158	1.187845692	0.3168735258
		RSDT2 Ref(b)	0.2451555605	1.187448435	0.3118723402
		Present	0.2451946715	1.187109491	0.3076738915
	4	RSDT1 Ref(b)	0.2676028572	1.298330162	0.3250024098
		RSDT2 Ref(b)	0.2676739215	1.297939361	0.3207031564
		Present	0.2677272719	1.297604584	0.3170722614
	5	RSDT1 Ref(b)	0.2829700265	1.373757679	0.3309424574
		RSDT2 Ref(b)	0.2830548580	1.373376155	0.3271941912
		Present	0.2831197749	1.373048061	0.3240047527

To demonstrate the accuracy of the present theory in predicting the bending responses of Al/Al_2O_3 plates some results are tabulated here for comparison with the available ones in the literature (Reddy *et al*. 2001, Cooke and Levinson 1983, Lee *et al*. 2002).

The center deflections under uniform loads (K_w=K_s=0) as shown in Tables 4.

The comparisons results for deflections of homogeneous plates resting on two-parameter elastic foundation under uniform loads are presented in Table 5. The present theory

Table 6 Continued.

	p	Method	$\widehat{w}$	$\bar{\sigma}_x$	$\bar{\tau}_{xz}$
1-2-1	0	RSDT1 Ref(b)	0.07790303811	1.995500426	0.2461800786
		RSDT2 Ref(b)	0.07790968813	1.995500426	0.2385722368
		Present	0.07790626339	1.993313666	0.2321588570
	1	RSDT1 Ref(b)	0.1349817311	0.6475971685	0.2705450198
		RSDT2 Ref(b)	0.1349767793	0.6472490279	0.2628693010
		Present	0.1349655957	0.6469555714	0.2565050040
	2	RSDT1 Ref(b)	0.1692408728	0.8158819124	0.2819062066
		RSDT2 Ref(b)	0.1692362771	0.8154785470	0.2745137059
		Present	0.1692265738	0.8151401001	0.2684288499
	3	RSDT1 Ref(b)	0.1903941485	0.9198385532	0.2881994693
		RSDT2 Ref(b)	0.1903936675	0.9194123216	0.2811258564
		Present	0.1903880701	0.9190551778	0.2753242467
	4	RSDT1 Ref(b)	0.2043026094	0.9882021870	0.2921729400
		RSDT2 Ref(b)	0.2043068289	0.9877663216	0.2853784402
		Present	0.2043055459	0.9874011732	0.2798160095
	5	RSDT1 Ref(b)	0.2139890657	1.035815027	0.2949192557
		RSDT2 Ref(b)	0.2139976337	1.035375225	0.2883554168
		Present	0.2140002193	1.035006687	0.2829869587
2-1-2	0	RSDT1 Ref(b)	0.07790303811	1.995500426	0.2461800786
		RSDT2 Ref(b)	0.07790968813	1.995500426	0.2385722368
		Present	0.07790626347	1.993313666	0.2321588570
	1	RSDT1 Ref(b)	0.1734597228	0.8353570262	0.3015504090
		RSDT2 Ref(b)	0.1734932520	0.8350075555	0.2951461351
		Present	0.1735128134	0.8347083932	0.2897240909
	2	RSDT1 Ref(b)	0.2432596500	1.177554594	0.3344535292
		RSDT2 Ref(b)	0.2433313416	1.177177220	0.3295841212
		Present	0.2433830725	1.176851545	0.3254000363
	3	RSDT1 Ref(b)	0.2872645148	1.393221446	0.3562078083
		RSDT2 Ref(b)	0.2873727377	1.392856605	0.3526990656
		Present	0.2874549794	1.392538447	0.3495973445
	4	RSDT1 Ref(b)	0.3148758215	1.528387607	0.3721411748
		RSDT2 Ref(b)	0.3150142476	1.528043627	0.3697033242
		Present	0.3151215501	1.527740512	0.3674435652
	5	RSDT1 Ref(b)	0.3328492117	1.616230779	0.3845927855
		RSDT2 Ref(b)	0.3330115755	1.615906291	0.3829703775
		Present	0.3331386274	1.615617583	0.3813446243
2-2-1	0	RSDT1 Ref(b)	0.07790303811	1.995500426	0.2461800786
		RSDT2 Ref(b)	0.07790968813	1.995500426	0.2385722368
		Present	0.07790626347	1.993313666	0.2321588570
	1	RSDT1 Ref(b)	0.1457900983	0.6551706776	0.2817627605
		RSDT2 Ref(b)	0.1457976301	0.6548254747	0.2743788976
		Present	0.1457959149	0.6545323869	0.2682002042
	2	RSDT1 Ref(b)	0.1894930926	0.8339863401	0.3002035928
		RSDT2 Ref(b)	0.1895109912	0.8335924793	0.2933103754
		Present	0.1895183739	0.8332580801	0.2875437341
	3	RSDT1 Ref(b)	0.2166927584	0.9434577978	0.3113186472
		RSDT2 Ref(b)	0.2167221065	0.9430467085	0.3048721239
		Present	0.2167391635	0.9426970178	0.2994666116
	4	RSDT1 Ref(b)	0.2343233353	1.013728625	0.3188535037
		RSDT2 Ref(b)	0.2343624668	1.013311427	0.3127535851
		Present	0.2343876708	1.012955788	0.3076232112
	5	RSDT1 Ref(b)	0.2463510788	1.061363472	0.3243713954
		RSDT2 Ref(b)	0.2463980407	1.060944155	0.3185308111
		Present	0.2464297130	1.060586039	0.3136038294

(b) Merdaci *et al*. (2011)

with only four unknowns gives excellent results in all cases with those of Zenkour and Radwan (2018).

Table 6 exhibit the dimensionless center deflection $\widehat{w}$, normal $\bar{\sigma}_x$ and shear stress $\bar{\tau}_{xz}$ for an FG sandwich plate

Table 7 Dimensionless deflection $\bar{w}$ of square plates (a/h=10)

Boundary conditions	p	Method	Scheme				
			1-0-1	2-1-2	1-1-1	2-2-1	1-2-1
SSSS	0	Abdelaziz *et al*. (2017)	0.2956	0.2956	0.2956	0.2956	0.2956
		Present	0,2960	0,2960	0,2960	0,2960	0,2960
	0.5	Abdelaziz *et al*. (2017)	0.5227	0.4846	0.4560	0.4366	0.4172
		Present	0,5229	0.4849	0.4564	0,4370	0.4177
	1	Abdelaziz *et al*. (2017)	0.7454	0.6593	0.5954	0.5537	0.5124
		Present	0.7452	0.6593	0.5956	0.5540	0.5129
	2	Abdelaziz *et al*. (2017)	1.0839	0.9254	0.8009	0.7200	0.6427
		Present	1.0830	0.9249	0.8008	0.7202	0.6431
	5	Abdelaziz *et al*. (2017)	1.4519	1.2678	1.0767	0.9367	0.8131
		Present	1.4492	1.2659	1.0758	0.9364	0.8132
	10	Abdelaziz *et al*. (2017)	1.5519	1.4053	1.2070	1.0392	0.8998
		Present	1.5489	1.4026	1.2055	1.0387	0.8996
CSCS	0	Abdelaziz *et al*. (2017)	0.1836	0.1836	0.1836	0.1836	0.1836
		Present	0.1875	0.1875	0.1875	0.1875	0.1875
	0.5	Abdelaziz *et al*. (2017)	0.3205	0.2972	0.2799	0.2682	0.2565
		Present	0.3251	0.3016	0.2842	0.2726	0.2608
	1	Abdelaziz *et al*. (2017)	0.4546	0.4020	0.3634	0.3384	0.3134
		Present	0,4595	0,4066	0,3678	0,3429	0,3179
	2	Abdelaziz *et al*. (2017)	0.6886	0.5615	0.4863	0.4379	0.3913
		Present	0,6637	0,5659	0,4908	0,4426	0,3960
	5	Abdelaziz *et al*. (2017)	0.8835	0.7670	0.6513	0.5676	0.4931
		Present	0,8891	0,7708	0,6554	0,5722	0,4977
	10	Abdelaziz *et al*. (2017)	0.9492	0.8503	0.7294	0.6290	0.5448
		Present	0,9569	0,8538	0,7331	0,6336	0,5494
CCCC	0	Abdelaziz *et al*. (2017)	0.1606	0.1606	0.1606	0.1606	0.1606
		Present	0,1595	0,1595	0,1595	0,1595	0,1595
	0.5	Abdelaziz *et al*. (2017)	0.2777	0.2576	0.2427	0.2327	0.2226
		Present	0,2766	0,2566	0,2418	0,2320	0,2219
	1	Abdelaziz *et al*. (2017)	0.3922	0.3468	0.3137	0.2924	0.2710
		Present	0,3908	0,3458	0,3129	0,2917	0,2705
	2	Abdelaziz *et al*. (2017)	0.5666	0.4825	0.4182	0.3770	0.3371
		Present	0,5641	0,4809	0,4171	0,3763	0,3367
	5	Abdelaziz *et al*. (2017)	0.7610	0.6577	0.5584	0.4873	0.4236
		Present	0,7557	0,6545	0,5566	0,4861	0,4229
	10	Abdelaziz *et al*. (2017)	0.8208	0.7292	0.6249	0.5396	0.4676
		Present	0,8139	0,7249	0,6224	0,5381	0,4667
FCFC	0	Abdelaziz *et al*. (2017)	0.1038	0.1038	0.1038	0.1038	0.1038
		Present	0.1027	0.1027	0.1027	0.1027	0.1027
	0.5	Abdelaziz *et al*. (2017)	0.1784	0.1655	0.1560	0.1496	0.1432
		Present	0.1771	0.1644	0.1550	0.1487	0.1423
	1	Abdelaziz *et al*. (2017)	0.2512	0.2221	0.2010	0.1875	0.1739
		Present	0.2497	0.2209	0.2000	0.1866	0.1731
	2	Abdelaziz *et al*. (2017)	0.3622	0.3082	0.2672	0.2411	0.2158
		Present	0.3598	0.3065	0.2660	0.2402	0.2150
	5	Abdelaziz *et al*. (2017)	0.4868	0.4195	0.3561	0.3110	0.2705
		Present	0.4821	0.4166	0.3543	0.3097	0.2696
	10	Abdelaziz *et al*. (2017)	0.5265	0.4651	0.3983	0.3442	0.2984
		Present	0.5203	0.4613	0.3960	0.3426	0.2973

subjected to a sinusoidal distributed load. The resultants obtained are compared with the solutions given by Merdaci *et al*. (2011). It can be seen that the obtained predictions for deflections are in good agreement. To demonstrate the accuracy of the present theory in predicting the bending responses of FG sandwich plates under various boundary conditions.

The comparisons between the obtained results and those developed by Abdelaziz *et al*. (2017) have been made in Table 7. It is apparent that the results of the present theory agree very well with those given by Abdelaziz *et al*. (2017).Table 7 provides the dimensionless values of the transverse deflections $\bar{w}$ of various types of powerly graded sandwich plates under various boundary conditions.

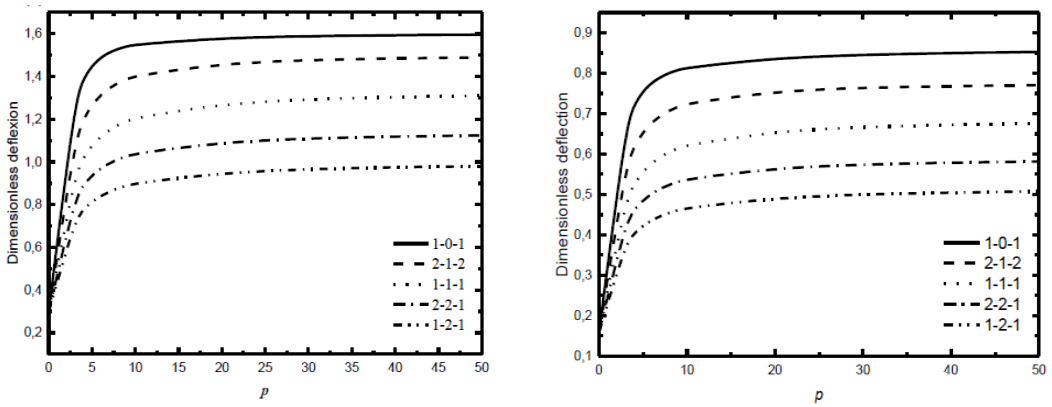

(a) simply supported plate (b) clamped plate

Fig. 2 Effect of the inhomogeneity parameter (p) on dimensionless deflection ($\bar{w}$) of square FG sandwich plates (a/h=10)

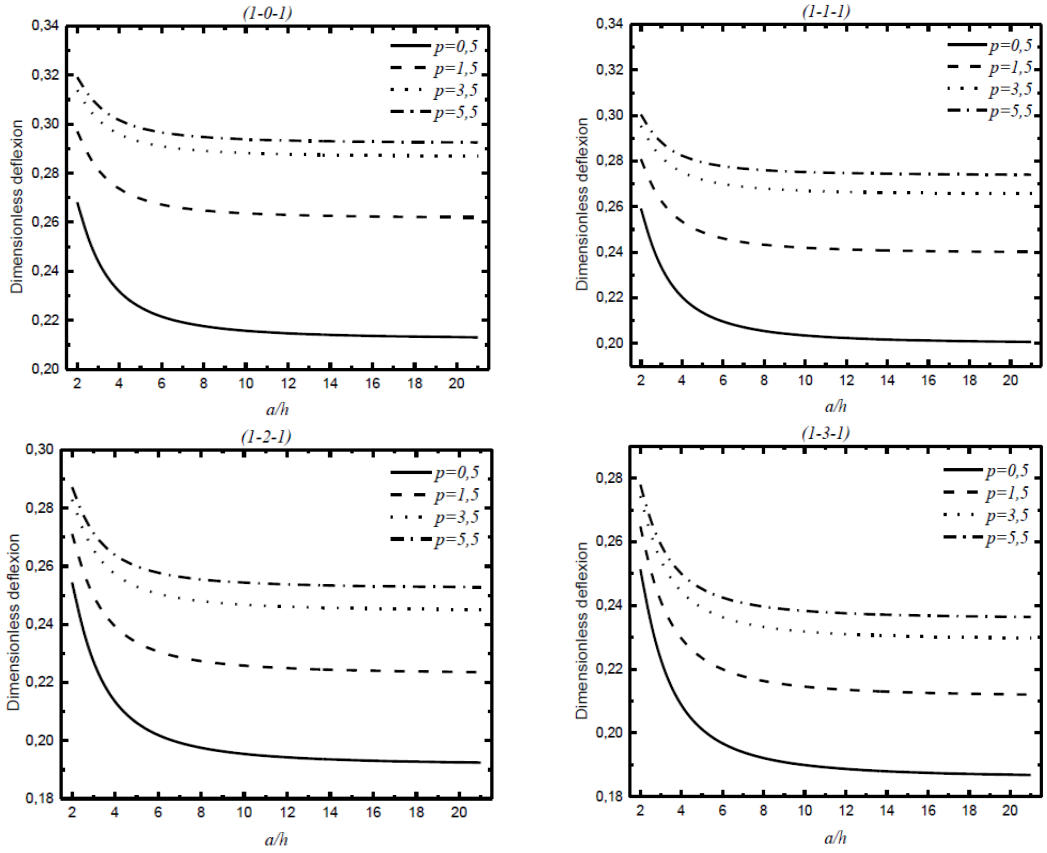

Fig. 3 Dimensionless center deflection $\bar{w}$ versus side-to-thickness ratio a/h FGM sandwich square plates on Elastic Foundations (K_w=100, K_s=10)

The results are compared with those obtained using hyperbolic shear deformation theory developed by Abdelaziz *et al*. (2017).

Good agreement is achieved between the present results obtained by using the present shear deformation theory and those of Zenkour and Radwan (2018) and Abdelaziz *et al*. (2017). It is remarked that the stiffer and softer plates correspond to the FCFC and SSSS ones, respectively. With the increase of the inhomogeneity parameter p, the plate becomes softer and hence, leads to an increase of deflection. This due to the fact that when the parameter p increases the plate tends to be metallic.

In Fig. 2, the variations of deflection of FG sandwich square plates versus the inhomogeneity parameter are presented, respectively. Different layer configurations are employed for multi-layered FGM plates. The thickness ratio of the plate is considered equal to 10. It can be observed that increasing the inhomogeneity parameter $p$leads to increase in deflection (Fig. 2). This behavior can be attributed to the fact that higher inhomogeneity parameter p corresponds to lower volume fraction of the ceramic phase. Thus, increasing the inhomogeneity parameter makes the plate softer because of the high portion of metal in comparison with the ceramic part, and consequently, results

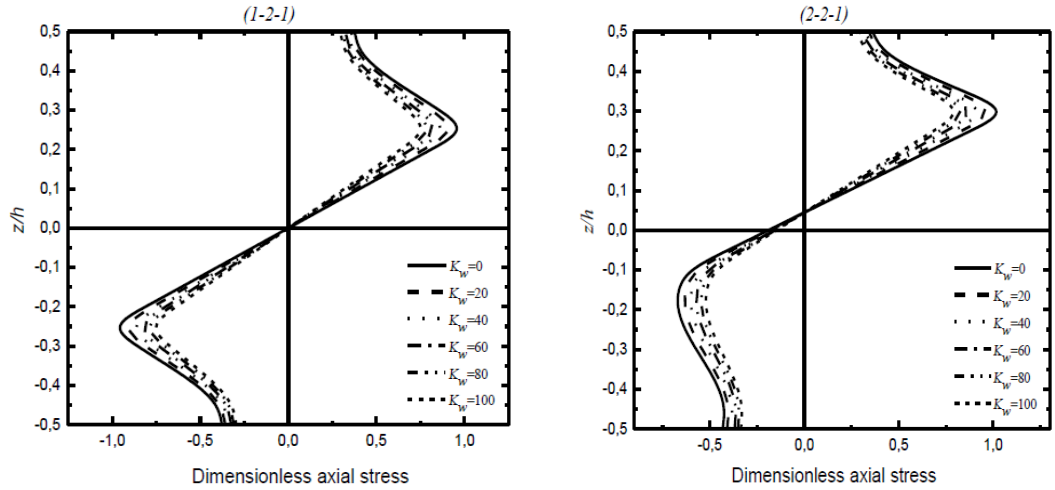

Fig. 4 The axial stress $\bar{\sigma}_x$ through the thickness of symmetric and unsymmetric simply-supported FGM sandwich square plates (p=2) for different values of Winkler modulus parameter K_w with K_s=10 and a/h=10

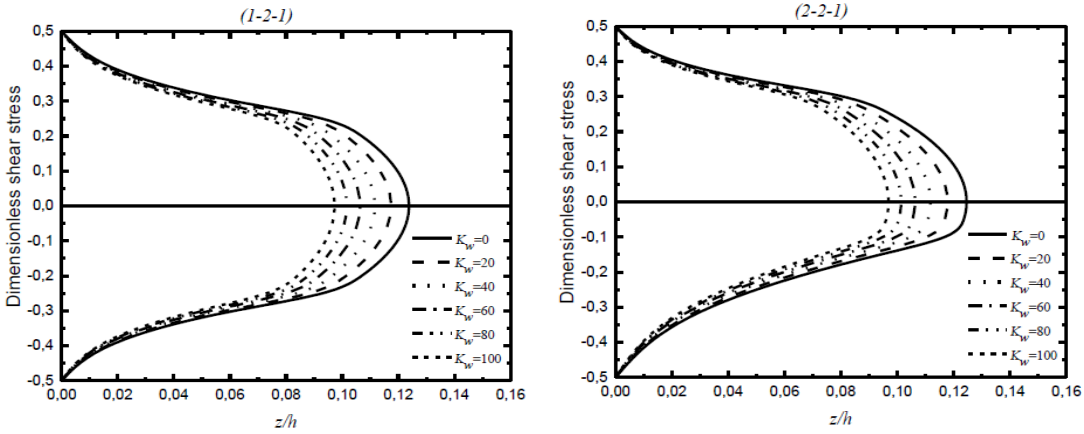

Fig. 5 The axial stress, $\bar{\tau}_{xz}$, through the thickness of symmetric and unsymmetric simply-supported FGM sandwich square plates (p=2) for different values of Winkler modulus parameter K_w with K_s=10 and a/h=10

in an increase in deflection. It is observed from results that the hardest and softest plates correspond to the (1-2-1) and (1-0-1) schemes, respectively. Such behavior is due to the fact that the (1-2-1) and (1-0-1) FG sandwich plates correspond to the highest and lowest volume fractions of the ceramic phase, and thus makes them become the hardest and softest ones. In addition, it can be seen from Fig. 2, that when clamped boundary conditions (CCCC) are considered, the plate becomes stiffer; this has led to a reduction of the deflection (Fig. 2(b)).

Fig. 3 shows the variation of the center deflection $\bar{w}$ with side-to-thickness ratio (a/h) for different types of FGM sandwich plates resting on Elastic Foundations (K_w=100, K_s=10). It can be seen that the center deflection $\bar{w}$ increase monotonically as p increases. It decreases with the increase of a/h ratios. The difference is almost constant with the increase of side-to-thickness ratio. It is also observed that the center deflection $\bar{w}$ is reduced as the thickness of the core increases.

Fig. 4 depict the through-the-thickness distributions of the axial stress $\bar{\sigma}_x$ in the FGM (p=2) square plates under the sinusoidal loads. As exhibited in Fig. 4 the axial stress, is compressive throughout the plate up to z/h=0 for symmetric FGM sandwich square plates and then they become tensile. On the other hand for unsymmetric FGM sandwich square plates, is compressive throughout the plate up to z/h=0.05 and then they become tensile.

The maximum compressive stresses occur at a point on the bottom surface and the maximum tensile stresses occur, of course, at a point on the top surface of the FGM sandwich plate. In addition, it can be seen from this figure that the elastic foundation has a significant effect on the maximum values of the axial stress. It is observed that normal stress ($\bar{\sigma}_x$) increases gradually with decreasing K_w.

Fig. 5 depict the through-the-thickness distributions of the shear stresses $\bar{\tau}_{xz}$ in the square FGM sandwich plate under sinusoidal distributed load. The volume fraction exponent of the FGM sandwich plate is taken as p=2 in this figure. It is observed that transverse shear stress ($\bar{\tau}_{xz}$) increases gradually with decreasing K_w.

It is indicated that large moduli of elastic foundation can enhance bending rigidity of the sandwich plate. It should be noted that the maximum value is reached at the center of the symmetrical FGM sandwich plate. But not at the center, in the case of the unsymmetric FGM sandwich plate.

The dimensionless deflection $\bar{w}$ of the (1-2-1) FGM

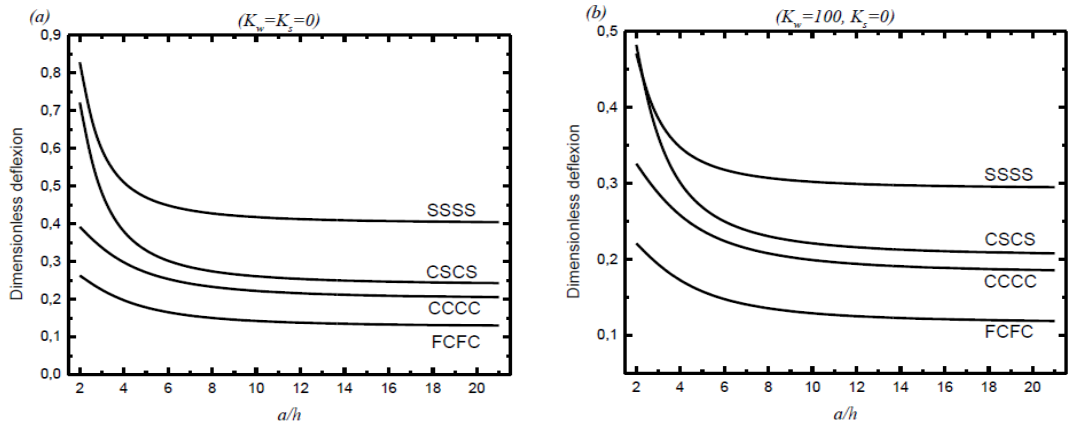

Fig. 6 dimensionless deflection $\overline{w}$ versus the side-to-thickness ratio a/h of the (1-2-1) FGM sandwich square Plate resting on Winkler's elastic foundation with various boundary conditions (p=*0.*5)

Table 8 Comparison of free vibration ($\frac{\omega b^2}{\pi^2}\sqrt{\rho h/D}$) of a simply supported homogeneous square plate (a/b=1, p=0) resting on Pasternak's elastic foundations (K_s=10)

m	n	b/h	K_w	Sobhy (2013)	Present
1	1	100	100	2.6551	2.6551
			500	3.3400	3.3400
		10	200	2.7842	2.7842
			1000	3.9806	3.9806
2	1	100	100	5.5718	5.5718
			500	5.9287	5.9287
		10	200	5.3051	5.3049
			1000	6.0085	6.0083
2	2	100	100	8.5405	8.5405
			500	8.7775	8.7775
		10	200	7.7311	7.7303
			1000	8.2237	8.2229

sandwich square plate resting on Winkler's elastic foundation with various boundary conditions are illustrated in Fig. 6. It is noted that $\overline{w}$ decrease gradually as the side-to-thickness ratio a/h increases. The result of the simply-supported sandwich plate is great than that of CCCC, CSCS and FCFC sandwich plate.

Fig. 7 illustrate the variations of dimensionless deflection as functions of the aspect ratio b/a of the SSSS and CCCC plate for various values of the elastic foundation parameters. The dimensionless deflection increase directly as b/a increases, as shown in Fig. 7. Obviously, the dimensionless deflection is increasing with the increasing of the foundation stiffnesses.

Free vibration analysis

The non-dimensionalized natural frequencies of general rectangular isotropic, and FG Al/Al2O3 plates are taken for comparison. Tables 8 and 9 give the nondimensionalized values of the natural frequencies for homogeneous isotropic plates (p=0) resting on elastic foundations. The results are compared with those obtained by Sobhy (2013). It can be seen that the present results are in good agreement with the solutions given by Sobhy (2013). It is also noted that the

Table 9 Comparison of free vibration ($\frac{\omega b^2}{\pi^2}\sqrt{\rho h/D}$) of a clamped homogeneous square plate (a/b=1, p=0) resting on Winkler's elastic foundation (m=n=1, h/b=0.015, v=0.15, K_s=0)

K_w	Sobhy (2013)	Present
1390.2	5.3330	5.3332
2780.4	6.5349	6.5351

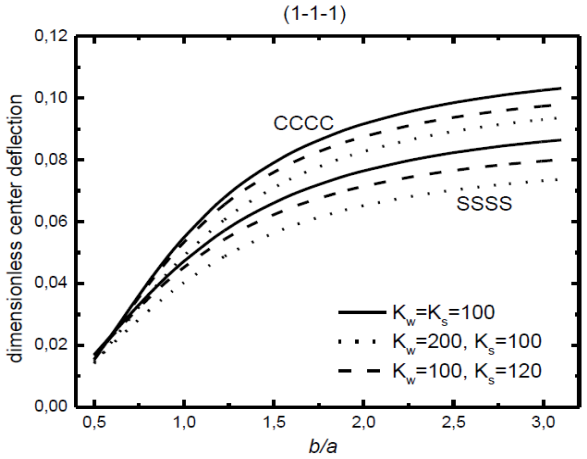

Fig. 7 dimensionless deflection $\overline{w}$ versus the aspect ratio b/a of simply-supported and clamped sandwich plate for different values of foundation stiffnesses K_w and K_s (a/h=10, p=5)

natural frequencies of simply-supported and clamped homogeneous square plates increase as Winkler's foundation parameter K_w increases.

Table 10 give the nondimensionalized values of the natural frequencies of various types of simply supported functionally graded sandwich square plates. The results are compared with those obtained using various shear deformation plate theories (Sobhy 2013). Good agreement is achieved between the present solutions and the published ones. It can be observed from Table 10 that the increase of the core thickness of the FGM sandwich plates leads to the increase of the frequencies, except for the case of the plates resting on Pasternak's foundations where the variation of

Table 10 Effects of elastic foundation stiffnesses K_w and K_s and side-to-thickness ratio a/h on the free vibration $\bar{\omega}$ of various types of simply supported sandwich square plates (p=1.5)

Scheme	Theory	k_w=k_s=0			k_w=100, k_s=0			k_w=100, k_s=100		
		a/h=5	10	20	a/h=5	10	20	a/h=5	10	20
1-0-1	FPT[c]	0,9547	1,0167	1,0347	1,4061	1,461	1,4775	4,7803	4,8851	4,9134
	TPT[c]	0,9647	1,0198	1,0356	1,4121	1,4631	1,4781	4,7807	4,8854	4,9135
	SPT[c]	0,9655	1,02	1,0356	1,4125	1,4633	1,4781	4,7808	4,8854	4,9135
	EPT[c]	0,9663	1,0203	1,0357	1,4131	1,4635	1,4782	4,7808	4,8854	4,9135
	HPT[c]	0,9643	1,0196	1,0355	1,4119	1,463	1,4781	4,7805	4,8854	4,9135
	Present	0,9600	1,0152	1,0310	1,4057	1,4566	1,4716	4,7600	4,8640	4,892
1-1-1	FPT[c]	1,0717	1,1367	1,1555	1,1563	1,5227	1,5401	4,6538	4,7513	4,7788
	TPT[c]	1,0807	1,1395	1,1563	1,4695	1,5247	1,5407	4,6537	4,7517	4,7789
	SPT[c]	1,0817	1,1396	1,1563	1,4697	1,5248	1,5407	4,6537	4,7517	4,7789
	EPT[c]	1,0815	1,1398	1,1563	1,47	1,5249	1,5407	4,6537	4,7517	4,779
	HPT[c]	1,0816	1,1398	1,1563	1,4703	1,5249	1,5407	4,6538	4,7518	4,779
	Present	1,0774	1,1363	1,1531	1,4652	1,5204	1,5364	4,6408	4,7386	4,7658
1-2-1	FPT[c]	1,0717	1,1367	1,1555	1,1563	1,5227	1,5401	4,6538	4,7513	4,7788
	TPT[c]	1,0807	1,1395	1,1563	1,4695	1,5247	1,5407	4,6537	4,7517	4,7789
	SPT[c]	1,0817	1,1396	1,1563	1,4697	1,5248	1,5407	4,6537	4,7517	4,7789
	EPT[c]	1,0815	1,1398	1,1563	1,47	1,5249	1,5407	4,6537	4,7517	4,779
	HPT[c]	1,0816	1,1398	1,1563	1,4703	1,5249	1,5407	4,6538	4,7518	4,779
	Present	1,0774	1,1363	1,1531	1,4652	1,5204	1,5364	4,6408	4,7386	4,7658
1-3-1	FPT[c]	1,2605	1,346	1,371	1,5912	1,6688	1,692	4,5914	4,6898	4,719
	TPT[c]	1,2666	1,348	1,3716	1,5956	1,6704	1,6924	4,5911	4,6901	4,7192
	SPT[c]	1,2663	1,3479	1,3716	1,5954	1,6703	1,6924	4,591	4,6901	4,7192
	EPT[c]	1,2662	1,3478	1,3715	1,5953	1,6703	1,6924	4,5909	4,69	4,7192
	HPT[c]	1,2753	1,3506	1,3723	1,6024	1,6724	1,693	4,5921	4,6907	4,7194
	Present	1,2648	1,3459	1,3694	1,5933	1,6678	1,6898	4,5836	4,6827	4,7118

[c]Sobhy (2013). EPT: exponential shear deformation plate theory; FPT: first-order shear deformation plate theory; HPT: hyperbolic shear deformation plate theory; SPT: sinusoidal shear deformation plate theory; TPT: third-order shear deformation plate theory

Table 11 Dimensionless fundamental frequency $\bar{\omega}$ of sandwich square plates (a/h=10) with various boundary conditions

Boundary conditions	p	Method	Scheme				
			1-0-1	2-1-2	1-1-1	2-2-1	1-2-1
SSSS	0	Abdelaziz *et al*. (2017)	0.2956	0.2956	0.2956	0.2956	0.2956
		Present	0,2960	0,2960	0,2960	0,2960	0,2960
	0.5	Abdelaziz *et al*. (2017)	0.5227	0.4846	0.4560	0.4366	0.4172
		Present	0,5229	0.4849	0.4564	0,4370	0.4177
	1	Abdelaziz *et al*. (2017)	0.7454	0.6593	0.5954	0.5537	0.5124
		Present	0.7452	0.6593	0.5956	0.5540	0.5129
	2	Abdelaziz *et al*. (2017)	1.0839	0.9254	0.8009	0.7200	0.6427
		Present	1.0830	0.9249	0.8008	0.7202	0.6431
	5	Abdelaziz *et al*. (2017)	1.4519	1.2678	1.0767	0.9367	0.8131
		Present	1.4492	1.2659	1.0758	0.9364	0.8132
	10	Abdelaziz *et al*. (2017)	1.5519	1.4053	1.2070	1.0392	0.8998
		Present	1.5489	1.4026	1.2055	1.0387	0.8996

them is reversed. In addition, the vibration frequencies are increasing with the existence of the elastic foundations. The inclusion of the Pasternak's foundation parameters gives results more than those with the inclusion of Winkler's foundation parameter.

Table 11 provides the nondimensionalized values of the natural frequencies $\bar{\omega}$ of various types of powerly graded sandwich plates under various boundary conditions. The results are compared with those obtained by Abdelaziz *et al*. (2017). Good agreement is achieved between the present results obtained by using the present refined theory with only a four-unknown and those of Abdelaziz *et al*. (2017). It is remarked that the stiffer and softer plates correspond to the FCFC and SSSS ones, respectively. With the increase of the inhomogeneity parameter p, the plate becomes softer and hence, leads to a reduction of the frequency. This due to the fact that when the parameter increases the plate tends to be metallic.

In Fig. 8, the variations of fundamental natural frequency of FG sandwich square plates versus the

Table 11 Continued

Boundary conditions	p	Method	Scheme				
			1-0-1	2-1-2	1-1-1	2-2-1	1-2-1
CSCS	0	Abdelaziz *et al*. (2017)	0.1836	0.1836	0.1836	0.1836	0.1836
		Present	0.1875	0.1875	0.1875	0.1875	0.1875
	0.5	Abdelaziz *et al*. (2017)	0.3205	0.2972	0.2799	0.2682	0.2565
		Present	0.3251	0.3016	0.2842	0.2726	0.2608
	1	Abdelaziz *et al*. (2017)	0.4546	0.4020	0.3634	0.3384	0.3134
		Present	0,4595	0,4066	0,3678	0,3429	0,3179
	2	Abdelaziz *et al*. (2017)	0.6886	0.5615	0.4863	0.4379	0.3913
		Present	0,6637	0,5659	0,4908	0,4426	0,3960
	5	Abdelaziz *et al*. (2017)	0.8835	0.7670	0.6513	0.5676	0.4931
		Present	0,8891	0,7708	0,6554	0,5722	0,4977
	10	Abdelaziz *et al*. (2017)	0.9492	0.8503	0.7294	0.6290	0.5448
		Present	0,9569	0,8538	0,7331	0,6336	0,5494
CCCC	0	Abdelaziz *et al*. (2017)	0.1606	0.1606	0.1606	0.1606	0.1606
		Present	0,1595	0,1595	0,1595	0,1595	0,1595
	0.5	Abdelaziz *et al*. (2017)	0.2777	0.2576	0.2427	0.2327	0.2226
		Present	0,2766	0,2566	0,2418	0,2320	0,2219
	1	Abdelaziz *et al*. (2017)	0.3922	0.3468	0.3137	0.2924	0.2710
		Present	0,3908	0,3458	0,3129	0,2917	0,2705
	2	Abdelaziz *et al*. (2017)	0.5666	0.4825	0.4182	0.3770	0.3371
		Present	0,5641	0,4809	0,4171	0,3763	0,3367
	5	Abdelaziz *et al*. (2017)	0.7610	0.6577	0.5584	0.4873	0.4236
		Present	0,7557	0,6545	0,5566	0,4861	0,4229
	10	Abdelaziz *et al*. (2017)	0.8208	0.7292	0.6249	0.5396	0.4676
		Present	0,8139	0,7249	0,6224	0,5381	0,4667

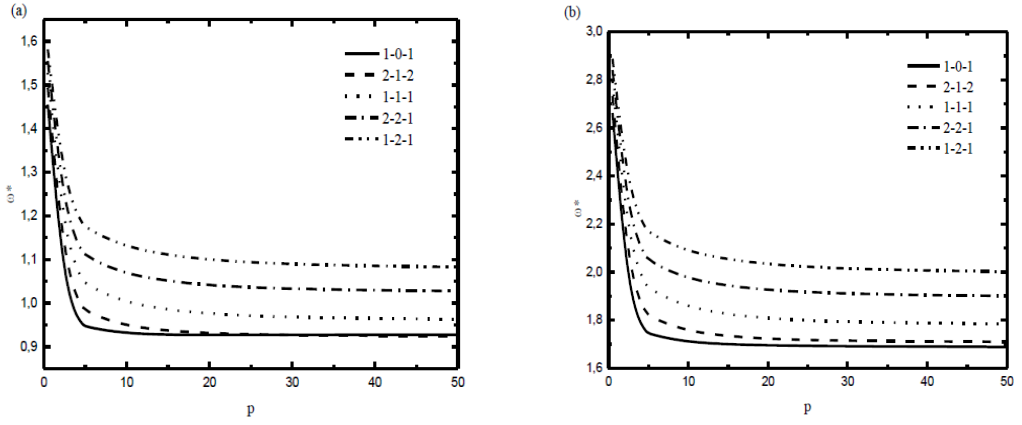

(a) simply supported plate (b) clamped plate

Fig. 8 Effect of the inhomogeneity parameter (p) on dimensionless frequency ($\bar{\omega}$) of square FG sandwich plates (a/h=10)

inhomogeneity parameter p are presented. Different layer configurations are employed for multi-layered FGM plates. The thickness ratio of the plate is considered equal to 10.

It can be observed that increasing the inhomogeneity parameter p leads to a reduction of natural frequency. This behavior can be attributed to the fact that higher inhomogeneity parameter p corresponds to lower volume fraction of the ceramic phase. Thus, increasing the inhomogeneity parameter makes the plate softer because of the high portion of metal in comparison with the ceramic part, and consequently, results in a reduction of natural frequency. It is observed from results that the hardest and softest plates correspond to the (1-2-1) and (1-0-1) schemes, respectively. Such behavior is due to the fact that the (1-2-1) and (1-0-1) FG sandwich plates correspond to the highest and lowest volume fractions of the ceramic phase, and thus makes them become the hardest and softest ones.

In addition, it can be seen, that when clamped boundary conditions (CCCC) are considered, the plate becomes stiffer; this has led to increasing the natural frequency.

Fig. 9 display the variations of the eigenfrequencies $\bar{\omega}$ the inhomogeneity parameter p. It can be seen that the frequencies $\bar{\omega}$ increase monotonically as p increases. It is also observed that the differences between curves are reduced as the core thickness increases.

The eigenfrequencies $\bar{\omega}$ of the (1-2-1) EGM sandwich square plate resting on Winkler's elastic foundation with various boundary conditions are illustrated in Fig. 10

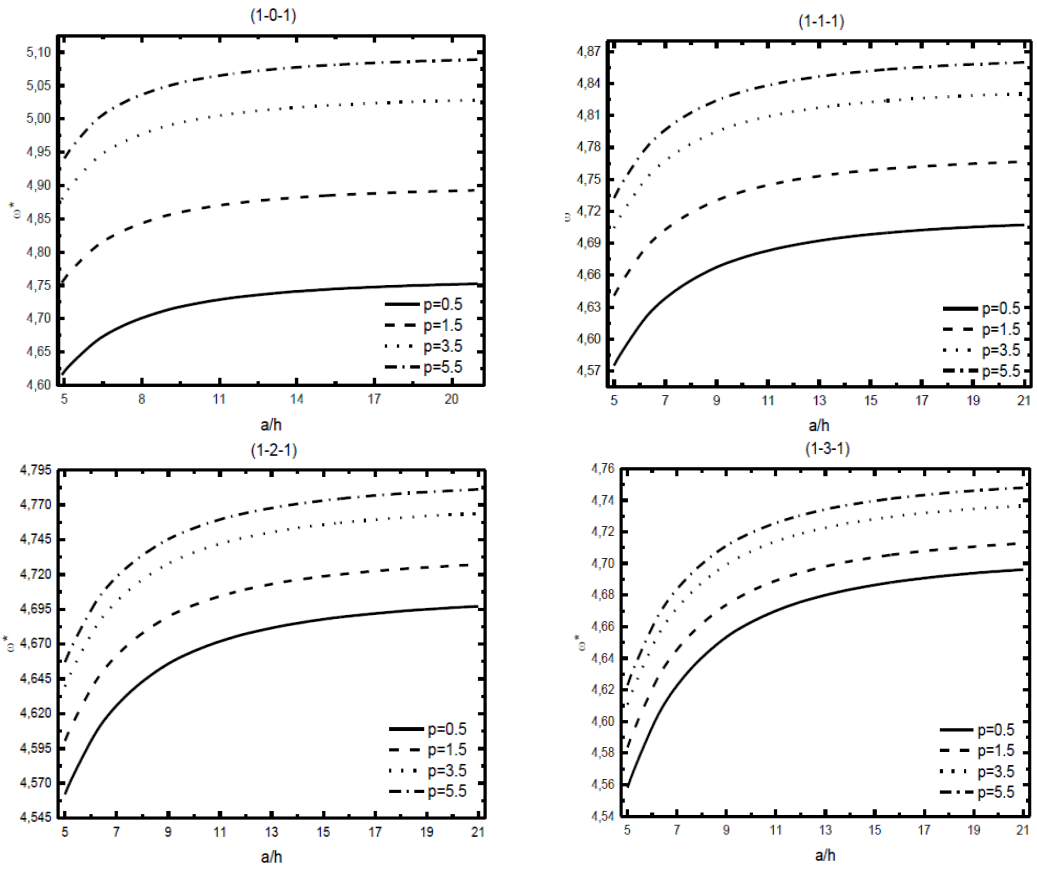

Fig. 9 Free vibration $\bar{\omega}$ versus the ratio *a/h* various values of the inhomogeneity parameter p and various types of simply-supported FGM sandwich square plates resting on elastic foundations (K_w=K_s=100)

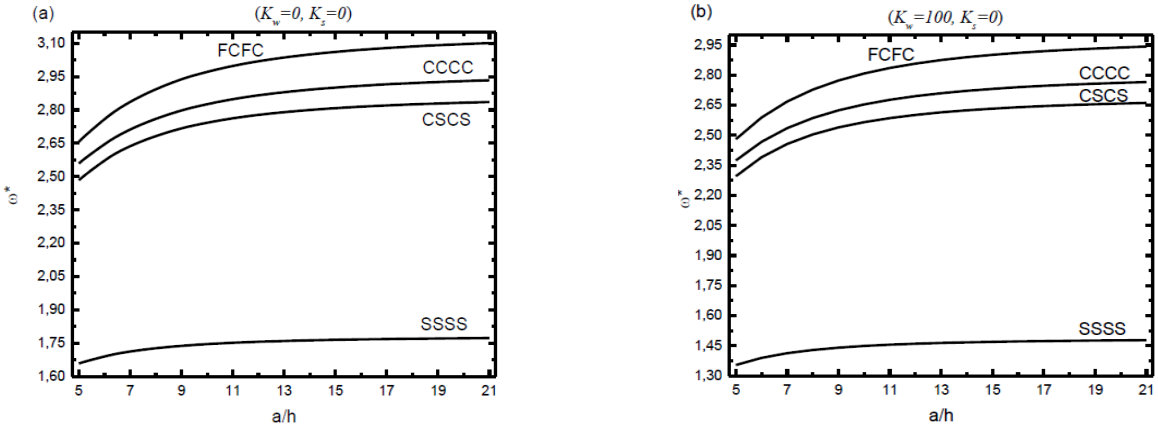

Fig. 10 Free vibration $\bar{\omega}$ versus the side-to-thickness ratio *a/h* of the (1-2-1) EGM sandwich square Plate resting on Winkler's elastic foundation with various boundary conditions (p=0.5)

without elastic foundation and resting on Winkler's elastic foundation, respectively. It is noted that $\bar{\omega}$ increase gradually as the side-to-thickness ratio *a/h* increases. The results of the simply-supported sandwich plate are less than that of the CCCC, CSCS and FCFC sandwich plate. For the FGM sandwich plate with intermediate boundary conditions, the results take the corresponding intermediate values.

Fig. 11 illustrate the variations of the natural frequencies as functions of the aspect ratio *b/a* of the SSSS and CCCC plate for various values of the elastic foundation parameters. As it is well known, the clamped boundary condition always overpredicts the vibration frequencies. The frequencies decrease directly as *b/a* increases. Obviously, the frequencies are increasing with the increasing of the foundation stiffnesses.

5. Conclusions

A new shear deformation theory for bending and free vibration analysis of various types of FGM sandwich a plate

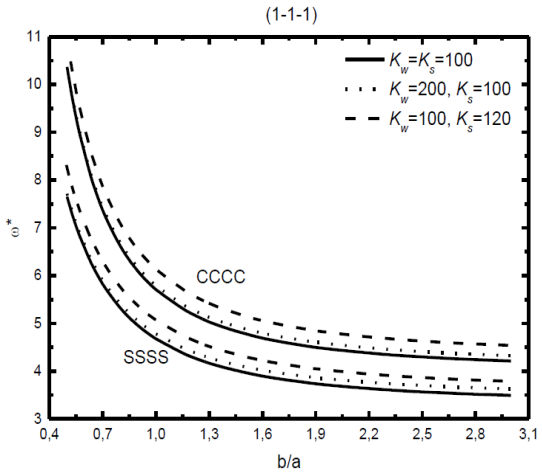

Fig. 11 Free vibration $\bar{\omega}$ versus the aspect ratio *b/a* of simply-supported and clamped sandwich plate for different values of foundation stiffnesses K_w and K_s (*a/h*=10, *p*=0.5)

with different cases of boundary conditions is proposed in this paper employing a simple hyperbolic shear deformation theory with only four unknowns. The sandwich plates are assumed to be leaned on two-parameter elastic foundations. Hamilton's principle is used herein to derive the equations of motion. To solve the problem for different boundary conditions, Galerkin's approach is utilized for symmetric and anti-symmertic FGM sandwich plates. The results obtained by the present formulation are compared with other results available in literature. Based on the results obtained, the following conclusions can be drawn from the present analysis:

1. The present results are very agreement with those being in literature.
2. The vibration frequencies for FG sandwich plates are generally lower than the corresponding values for homogeneous ceramic plates, while the deflections are higher than those of homogeneous ceramic plates.
3. The vibration frequencies increase as the side-to-thickness ratio increases, while the deflections decrease.
4. The vibration frequencies for simply supported powerly graded sandwich plates are lower than those for free and clamped powerly graded sandwich plates.
5. The deflections for simply supported powerly graded sandwich plates are higher than those for free and clamped powerly graded sandwich plates.

References

Abdelaziz, H.H., Meziane, M.A.A, Bousahla, A.A., Tounsi, A., Mahmoud, S.R. and Alwabli, A.S. (2017), "An efficient hyperbolic shear deformation theory for bending, buckling and free vibration of FGM sandwich plates with various boundary conditions", *Steel Compos. Struct.*, **25**(6), 693-704. https://doi.org/10.12989/scs.2017.25.6.693.

Abdelmalek, A., Bouazza, M., Zidour, M. and Benseddiq, N. (2019), "Hygrothermal effects on the free vibration behavior of composite plate using nth-order shear deformation theory: A micromechanical approach", *Iran J. Sci. Technol. Tran. Mech. Eng.*, **43**, 61-73. https://doi.org/10.1007/s40997-017-0140-y.

Abdelrahman, A.A., Eltaher, M.A., Kabeel, A.M., Abdraboh, A.M. and Hendi, A.A. (2019), "Free and forced analysis of perforated beams", *Steel Compos. Struct.*, **31**(5), 489-502. https://doi.org/10.12989/scs.2019.31.5.489.

Abdou, M.A., Othman, M.I.A., Tantawi, R.S. and Mansour, N.T. (2019), "Exact solutions of generalized thermoelastic medium with double porosity under L-S theory", *Ind. J. Phys.*, 1-12. https://doi.org/10.1007/s12648-019-01505-8.

Abrate S. (2008), "Functionally graded plates behave like homogeneous plates", *Compos. Part B: Eng.*, **39**, 151-158. https://doi.org/10.1016/j.compositesb.2007.02.026.

Akbaş Ş.D. (2018), "Forced vibration analysis of functionally graded porous deep beams", *Compos. Struct.*, **186**, 293-302. https://doi.org/10.1016/j.compstruct.2017.12.013.

Akbaş, S.D (2019a), "Nonlinear static analysis of laminated composite beams under hygro-thermal effect", *Struct. Eng. Mech.*, **72**(4), 433-441. https://doi.org/10.12989/sem.2019.72.4.433.

Akbaş, S.D. (2017), "Vibration and static analysis of functionally graded porous plates", *J. Appl. Comput. Mech.*, **3**(3), 199-207. https://doi.org/10.22055/JACM.2017.21540.1107.

Akbas, S.D. (2019b), "Forced vibration analysis of functionally graded sandwich deep beams", *Couple. Syst. Mech.*, **8**(3), 259-271. https://doi.org/10.12989/csm.2019.8.3.259.

Al-Maliki, A.F., Faleh, N.M. and Alasadi, A.A. (2019), "Finite element formulation and vibration of nonlocal refined metal foam beams with symmetric and non-symmetric porosities", *Struct. Monit. Mainten.*, **6**(2), 147-159. https://doi.org/10.12989/smm.2019.6.2.147.

Al-Osta, M.A. (2019), "Shear behaviour of RC beams retrofitted using UHPFRC panels epoxied to the sides", *Comput. Concrete*, **24**(1), 37-49. https://doi.org/10.12989/cac.2019.24.1.037.

Alasadi, A.A., Ahmed, R.A. and Faleh, N.M. (2019), "Analyzing nonlinear vibrations of metal foam nanobeams with symmetric and non-symmetric porosities", *Adv. Aircraf. Spacecraf. Sci.*, **6**(4), 273-282. https://doi.org/10.12989/aas.2019.6.4.273.

Arani, A.J. and Kolahchi, R. (2016), "Buckling analysis of embedded concrete columns armed with carbon nanotubes", *Comput. Concrete*, **17**(5), 567-578. https://doi.org/10.12989/cac.2016.17.5.567.

Arefi, M. (2015), "The effect of different functionalities of FGM and FGPM layers on free vibration analysis of the FG circular plates integrated with piezoelectric layers", *Smart Struct. Syst.*, **15**, 1345-1362. https://doi.org/10.12989/sss.2015.15.5.1345.

Avcar, M. (2019), "Free vibration of imperfect sigmoid and power law functionally graded beams", *Steel Compos. Struct.*, **30**(6), 603-615. https://doi.org/10.12989/scs.2019.30.6.603.

Barati, M.R. and Shahverdi, H. (2020), "Finite element forced vibration analysis of refined shear deformable nanocomposite graphene platelet-reinforced beams", *J. Brazil Soc. Mech. Sci. Eng.*, **42**(1), 33. https://doi.org/10.1007/s40430-019-2118-8.

Belmahi, S., Zidour, M. and Meradjah, M. (2019), "Small-scale effect on the forced vibration of a nano beam embedded an elastic medium using nonlocal elasticity theory", *Adv. Aircraf. Spacecraf. Sci.*, **6**(1), 1-18. https://doi.org/10.12989/aas.2019.6.1.001.

Belmahi, S., Zidour, M., Meradjah, M., Bensattalah, T. and Dihaj, A. (2018), "Analysis of boundary conditions effects on vibration of nanobeam in a polymeric matrix", *Struct. Eng. Mech.*, **67**(5), 517-525. https://doi.org/10.12989/sem.2018.67.5.517.

Benferhat, R., HassaineDaouadji, T., Hadji, L. and Said Mansour, M. (2016), "Static analysis of the FGM plate with porosities", *Steel Compos. Struct.*, **21**(1), 123-136. https://doi.org/10.12989/scs.2016.21.1.123.

Bensattalah, T., Zidour, M. and Daouadji, T.H. (2019), "A new nonlocal beam model for free vibration analysis of chiral single-walled carbon nanotubes", *Compos. Mater. Eng.*, **1**(1), 21-31. https://doi.org/10.12989/cme.2019.1.1.021.

Bensattalah, T., Zidour, M. and Hassaine Daouadji, T. (2018), "Analytical analysis for the forced vibration of CNT surrounding elastic medium including thermal effect using nonlocal Euler-Bernoulli theory", *Adv. Mater. Res*., **7**(3), 163-174. https://doi.org/10.12989/amr.2018.7.3.163.

Cooke, D.W. and Levinson, M. (1983), "Thick rectangular plates-II, the generalized Lévy solution", *Int. J. Mech. Sci.*, **25**(3), 207-215. https://doi.org/10.1016/0020-7403(83)90094-2.

Darilmaz, K. (2015), "Vibration analysis of functionally graded material (FGM) grid systems", *Steel Compos. Struct.*, **18**, 395-408. https://doi.org/10.12989/scs.2015.18.2.395.

Dihaj, A., Zidour, M., Meradjah, M., Rakrak, K., Heireche, H. and Chemi, A. (2018), "Free vibration analysis of chiral double-walled carbon nanotube embedded in an elastic medium using non-local elasticity theory and Euler Bernoulli beam model", *Struct. Eng. Mech*., **65**(3), 335-342. https://doi.org/10.12989/sem.2018.65.3.335.

Ebrahimi, F. and Barati, M.R. (2017a), "Vibration analysis of nonlocal strain gradient embedded single-layer graphene sheets under nonuniform in-plane loads", *J. Vib. Control*, 107754631773408. https://doi.org/10.1177/1077546317734083.

Ebrahimi, F. and Barati, M.R. (2017b), "Scale-dependent effects on wave propagation in magnetically affected single/double-layered compositionally graded nanosize beams", *Wave. Random Complex Media*, **28**(2), 326-342. https://doi.org/10.1080/17455030.2017.1346331.

Ebrahimi, F. and Barati, M.R. (2019), "A nonlocal strain gradient mass sensor based on vibrating hygro-thermally affected graphene nanosheets", *Iran J. Sci. Technol. Tran. Mech. Eng*., **43**, 205-220. https://doi.org/10.1007/s40997-017-0131-z.

Eltaher, M.A. and Mohamed, S.A. (2020), "Buckling and stability analysis of sandwich beams subjected to varying axial loads", *Steel Compos. Struct.*, **34**(2), 241-260. https://doi.org/10.12989/scs.2020.34.2.241.

Eltaher, M.A., Agwa, M. and Kabeel, A (2018), "Vibration analysis of material size-dependent CNTs using energy equivalent model", *J. Appl. Comput. Mech.*, **4**(2), 75-86. https://doi.org/10.22055/JACM.2017.22579.1136.

Eltaher, M.A., El-Borgi, S. and Reddy, J.N. (2016), "Nonlinear analysis of size-dependent and material-dependent nonlocal CNTs", *Compos. Struct.*, **153**, 902-913. https://doi.org/10.1016/j.compstruct.2016.07.013.

Eltaher, M.A., Fouda, N., El-midany, T. and Sadoun, A.M. (2018), "Modified porosity model in analysis of functionally graded porous nanobeams", *J. Brazil. Soc. Mech. Sci. Eng.*, **40**, 141. https://doi.org/10.1007/s40430-018-1065-0.

Eltaher, M.A., Mohamed, S.A. and Melaibari, A. (2020), "Static stability of a unified composite beams under varying axial loads", *Thin Wall. Struct*., **147**, 106488. https://doi.org/10.1016/j.tws.2019.106488.

Eltaher, M.A., Wagih, A., Melaibari, A., Fathy, A. and Lubineau, G. (2019), "Effect of Al_2O_3 particles on mechanical and tribological properties of Al-Mg dual-matrix nanocomposites", *Ceram. Int.*, **46**(5), 5779-5787. https://doi.org/10.1016/j.ceramint.2019.11.028.

Fadoun, O.O., Borokinni, A.S., Layeni, O.P. and Akinola, A.P. (2017), "Dynamics analysis of a transversely isotropic non-classical thin plate", *Wind Struct.*, **25**(1), 25-38. https://doi.org/10.12989/was.2017.25.1.025.

Faleh, N.M., Ahmed, R.A. and Fenjan, R.M. (2018), "On vibrations of porous FG nanoshells", *Int. J. Eng. Sci.*, **133**, 1-14. https://doi.org/10.1016/j.ijengsci.2018.08.007.

Fenjan, R.M., Ahmed, R.A., Alasadi, A.A. and Faleh, N.M. (2019), "Nonlocal strain gradient thermal vibration analysis of double-coupled metal foam plate system with uniform and non-uniform porosities", *Coupl. Syst. Mech*., **8**(3), 247-257. https://doi.org/10.12989/csm.2019.8.3.247.

Ghorbanpour, A.A., Cheraghbak, A. and Kolahchi, R. (2016), "Dynamic buckling of FGM viscoelastic nano-plates resting on orthotropic elastic medium based on sinusoidal shear deformation theory", *Struct. Eng. Mech.*, **60**, 489-505. https://doi.org/10.12989/sem.2016.60.3.489.

Giunta, G., Belouettar, S. and Ferreira, A.J.M. (2016), "A static analysis of three-dimensional functionally graded beams by hierarchical modelling and a collocation meshless solution method", *Acta Mechanica*, **227**(4), 969-991. https://doi.org/10.1007/s00707-015-1503-3.

Goldsmith, W., Wang, G., Li, K. and Crane, D. (1997), "Perforation of cellular sandwich plates", *Int. J. Impact Eng.*, **19**(5-6), 361-379. https://doi.org/10.1016/S0734-743X(97)00003-1.

Haciyev, V.C., Sofiyev, A.H. and Kuruoglu, N. (2018), "Free bending vibration analysis of thin bidirectionally exponentially graded orthotropic rectangular plates resting on two-parameter elastic foundations", *Compos. Struct*., **184**, 372-377. https://doi.org/10.1016/j.compstruct.2017.10.014.

Hadji, L., Zouatnia, N. and Bernard, F. (2019), "An analytical solution for bending and free vibration responses of functionally graded beams with porosities: Effect of the micromechanical models", *Struct. Eng. Mech.*, **69**(2), 231-241. https://doi.org/10.12989/sem.2019.69.2.231.

Hajmohammad, M.H., Zarei, M.S., Nouri, A. and Kolahchi, R. (2017), "Dynamic buckling of sensor/functionally graded-carbon nanotube-reinforced laminated plates/actuator based on sinusoidal-visco-piezoelasticity theories", *J. Sandw. Struct. Mater.*, 1099636217720373. https://doi.org/10.1177/1099636217720373.

Hamed, M.A., Salwa, A., Mohamed, S.A., Mohamed, A. and Eltaher, M.A, (2020), "Buckling analysis of sandwich beam rested on elastic foundation and subjected to varying axial in-plane loads", *Steel Compos. Struct*., **34**(1), 75-89. https://doi.org/10.12989/scs.2020.34.1.075.

Hamidi, A., Zidour, M., Bouakkaz, K. and Bensattalah, T. (2018), "Thermal and small-scale effects on vibration of embedded armchair single-walled carbon nanotubes", *J. Nano Res*., **51**, 24-38. https://doi.org/10.4028/www.scientific.net/JNanoR.51.24.

He, X.Q., Ng, T.Y., Sivashanker, S. and Liew, K.M. (2001), "Active control of FGM plates with integrated piezoelectric sensors and actuators", *Int. J. Solid. Struct.*, **38**, 1641-1655. https://doi.org/10.1016/S0020-7683(00)00050-0.

Hussain, M. and Naeem, M.N. (2019), "Effects of ring supports on vibration of armchair and zigzag FGM rotating carbon nanotubes using Galerkin's method", *Compos. Part B: Eng.*, **163**, 548-561. https://doi.org/10.1016/j.compositesb.2018.12.144.

Jha, D.K., Kant, T. and Singh, R.K. (2012), "Higher order shear and normal deformation theory for natural frequency of functionally graded rectangular plates", *Nucl. Eng. Des.*, **250**, 8-13. https://doi.org/10.1016/j.nucengdes.2012.05.001.

Kar, V.R. and Panda, S.K. (2015a), "Thermoelastic analysis of functionally graded doubly curved shell panels using nonlinear finite element method", *Compos. Struct*., **129**, 202-212. https://doi.org/10.1016/j.compstruct.2015.04.006.

Kar, V.R. and Panda, S.K. (2015b), "Large deformation bending analysis of functionally graded spherical shell using FEM", *Struct. Eng. Mech*., **53**(4), 661-679. https://doi.org/10.12989/sem.2015.53.4.661.

Kar, V.R. and Panda, S.K. (2015c), "Nonlinear flexural vibration of shear deformable functionally graded spherical shell panel", *Steel Compos. Struct*., **18**(3), 693-709. https://doi.org/10.12989/scs.2015.18.3.693.

Kar, V.R. and Panda, S.K. (2016), "Nonlinear thermomechanical behavior of functionally graded material Cylindrical/Hyperbolic/Elliptical shell panel with temperature-dependent and temperature-independent properties", *J. Press. Ves. Technol*., **138**(6), 061202. https://doi.org/10.1115/1.4033701.

Kar, V.R. and Panda, S.K. (2017), "Large-amplitude vibration of functionally graded Doubly-Curved panels under heat conduction", *AIAA J.*, **55**(12), 4376-4386. https://doi.org/10.2514/1.j055878.

Kar, V.R., Mahapatra, T.R. and Panda, S.K. (2015), "Nonlinear flexural analysis of laminated composite flat panel under hygro-thermo-mechanical loading", *Steel Compos. Struct.*, **19**(4),1011-1033. https://doi.org/10.12989/scs.2015.19.4.1011.

Katariya, P., Panda, S. and Mahapatra, T. (2018), "Bending and vibration analysis of skew sandwich plate", *Aircraf. Eng. Aerosp. Technol.*, **90**(6), 885-895. https://doi.org/10.1108/AEAT-05-2016-0087.

Katariya, P.V. and Panda, S.K. (2019a), "Numerical frequency analysis of skew sandwich layered composite shell structures under thermal environment including shear deformation effects", *Struct. Eng. Mech.*, **71**(6), 657-668. https://doi.org/10.12989/sem.2019.71.6.657.

Katariya, P.V. and Panda, S.K. (2019b), "Frequency and deflection responses of shear deformable skew sandwich curved shell panel: A finite element approach", *Arab. J. Sci. Eng.*, **44**(2), 1631-1648. https://doi.org/10.1007/s13369-018-3633-0.

Katariya, P.V., Hirwani, C.K. and Panda, S.K. (2019), "Geometrically nonlinear deflection and stress analysis of skew sandwich shell panel using higher-order theory", *Eng. Comput.*, **35**, 467-485. https://doi.org/10.1007/s00366-018-0609-3.

Katariya, P.V., Panda, S.K. and Mahapatra, T.R. (2017), "Prediction of nonlinear eigenfrequency of laminated curved sandwich structure using higher-order equivalent single-layer theory", *J. Sandw. Struct. Mater.*, 109963621772842. https://doi.org/10.1177/1099636217728420.

Kolahchi, R., Keshtegar, B. and Fakhar, M.H. (2020), "Optimization of dynamic buckling for sandwich nanocomposite plates with sensor and actuator layer based on sinusoidal-visco-piezoelasticity theories using Grey Wolf algorithm", *J. Sandw. Struct. Mater.*, **22**(1), 3-27. https://doi.org/10.1177/1099636217731071.

Kolahchi, R., Safari, M. and Esmailpour, M. (2016), "Dynamic stability analysis of temperature-dependent functionally graded CNT-reinforced visco-plates resting on orthotropic elastomeric medium", *Compos. Struct.*, **150**, 255-265. https://doi.org/10.1016/j.ijmecsci.2017.06.039.

Kolahchi, R., Zarei, M.S., Hajmohammad, M.H. and Nouri, A. (2017a), "Wave propagation of embedded viscoelastic FG-CNT-reinforced sandwich plates integrated with sensor and actuator based on refined zigzag theory", *Int. J. Mech. Sci.*, **130**, 534-545. https://doi.org/10.1016/j.ijmecsci.2017.06.039.

Kolahchi, R., Zarei, M.S., Hajmohammad, M.H. and Nouri, A. (2017b), "Wave propagation of embedded viscoelastic FG-CNT-reinforced sandwich plates integrated with sensor and actuator based on refined zigzag theory", *Int. J. Mech. Sci.*, **130**, 534-545. https://doi.org/10.1016/j.ijmecsci.2017.06.039.

Kunche, M.C., Mishra, P.K., Nallala, H.B., Hirwani, C.K., Katariya, P.V., Panda, S. and Panda, S.K. (2019), "Theoretical and experimental modal responses of adhesive bonded T-joints", *Wind Struct.*, **29**(5), 361-369. https://doi.org/10.12989/was.2019.29.5.361.

Lee, K.H., Lim, G.T. and Wang, C.M. (2002), "Thick Lévy plates revisited", *Int. J. Solid. Struct.*, **39**, 127-144. https://doi.org/10.1016/S0020-7683(01)00205-0

Liu, Y. (2011), "A refined shear deformation plate theory", *Int. J. Comput. Meth. Eng. Sci. Mech.*, **12**, 141-149. https://doi.org/10.1080/15502287.2011.564267.

Majeed, W.I. and Abdul Kareem Abed, Z. (2019)," Buckling and pre-stressed dynamics analysis of laminated composite plate with different boundary conditions", *Al-Khwarizmi Eng. J.*, **15**(1), 46-55. https://doi.org/10.22153/kej.2019.07.002.

Majeed, W.I. and Ghani, R.A. (2017), "Free vibration analysis of laminated composite plates with general elastic boundary supports", *J. Eng.*, **23**(4),100-124.

Mehar, K., Panda, S.K., Dehengia, A. and Kar, V.R. (2015), "Vibration analysis of functionally graded carbon nanotube reinforced composite plate in thermal environment", *J. Sandw. Struct. Mater.*, **18**(2), 151-173. https://doi.org/10.1177/1099636215613324.

Mehar, K., Panda, S.K., Devarajan, Y. and Choubey, G. (2019), "Numerical buckling analysis of graded CNT-reinforced composite sandwich shell structure under thermal loading", *Compos. Struct.*, **216**, 406-414. https://doi.org/10.1016/j.compstruct.2019.03.002.

Merdaci, S., Tounsi, A., Houari, M.S.A., Mechab, I., Hebali, H. and Benyoucef, S. (2011), "Two new refined shear displacement models for functionally graded sandwich plates", *Arch. Appl. Mech.*, **81**(11), 1507-1522. https://doi.org/10.1007/s00419-010-0497-5.

Mirjavadi, S.S., Forsat, M., Nikookar, M., Barati, M.R. and Hamouda, A.M.S. (2019b), "Nonlinear forced vibrations of sandwich smart nanobeams with two-phase piezo-magnetic face sheets", *Eur. Phys. J. Plus.,* **134**, 508. https://doi.org/10.1140/epjp/i2019-12806-8.

Mohamed, N., Mohamed, A., Eltaher, M.A., Mohamed, S.A and Seddek. L.F. (2019), "Energy equivalent model in analysis of postbuckling of imperfect carbon nanotubes resting on nonlinear elastic foundation", *Struct. Eng. Mech.*, **70**(6), 737-750. https://doi.org/10.12989/sem.2019.70.6.737.

Mouli, C.B., Ramji, K., Kar, V.R., Panda, S.K., Anil, L.K. and Pandey, H.K. (2018), "Numerical study of temperature dependent eigenfrequency responses of tilted functionally graded shallow shell structures", *Struct. Eng. Mech.*, **68**(5), 527-536. https://doi.org/10.12989/sem.2018.68.5.527.

Neves, A.M.A., Ferreira, A.J.M., Carrera, E., Cinefra, M., Jorge, R.M.N., MotaSoares, C.M. and Araújo, A.L. (2017), "Influence of zig-zag and warping effects on buckling of functionally graded sandwich plates according to sinusoidal shear deformation theories", *Mech. Adv. Mater. Struct.*, **24**(5), 360-376. https://doi.org/10.1080/15376494.2016.1191095.

Nguyen-Xuan, H., Thai, C.H. and Nguyen-Thoi, T. (2013), "Isogeometric finite element analysis of composite sandwich plates using a higher order shear deformation theory", *Compos. Part B: Eng.*, **55**, 558-574. https://doi.org/10.1016/j.compositesb.2013.06.044.

Nguyen, H.X., Nguyen, T.N., Abdel-Wahab, M., Bordas, S.P.A., Nguyen Xuan, H. and Vo, T.P. (2017), "A refined quasi-3D isogeometric analysis for functionally graded microplates based on the modified couple stress theory", *Comput. Meth. Appl. Mech. Eng.*, **313**, 904-940. https://doi.org/10.1016/j.cma.2016.10.002.

Nguyen, N.D., Nguyen, T.K., Nguyen, T.N. and Thai, H.T. (2018), "New Ritz-solution shape functions for analysis of thermo-mechanical buckling and vibration of laminated composite beams", *Compos. Struct.*, **184**, 452-460. https://doi.org/10.1016/j.compstruct.2017.10.003.

Nguyen, N.T., Hui, D., Lee, J. and Nguyen-Xuan, H. (2015), "An efficient computational approach for size-dependent analysis of functionally graded nanoplates", *Comput. Meth. Appl. Mech. Eng.*, **297**, 191-218. https://doi.org/10.1016/j.cma.2015.07.021.

Nguyen, V.H, Nguyen, T.K., Thai, H.T. and Vo, T.P. (2014), "A new inverse trigonometric shear deformation theory for isotropic and functionally graded sandwich plates", *Compos. Part B: Eng.*, **66**, 233-246. https://doi.org/10.1016/j.compositesb.2014.05.012.

Othman, M.I.A. and Lotfy, K. (2009), "Two-dimensional problem of generalized Magneto-Thermoelasticity with temperature dependent elastic moduli for different theories", *Multidisc. Model. Mater. Struct.*, **5**(3), 235-242.

https://doi.org/10.1163/157361109789016961.
Pandey, H.K., Hirwani, C.K., Sharma, N., Katariya, P.V. and Panda, S.K. (2019), "Effect of nano glass cenosphere filler on hybrid composite eigenfrequency responses-An FEM approach and experimental verification", *Adv. Nano Res.,* **7**(6), 419-429. https://doi.org/10.12989/anr.2019.7.6.419.
Panjehpour, M., Loh, E.W.K. and Deepak, T.J. (2018), "Structural insulated panels: State-of-the-Art", *Trend. Civil Eng. Arch.*, **3**(1) 336-340. https://doi.org/10.32474/TCEIA.2018.03.000151.
Pradhan, K.K. and Chakraverty, S. (2015), "Free vibration of functionally graded thin elliptic plates with various edge supports", *Struct. Eng. Mech.*, **53**, 337-354. https://doi.org/10.12989/sem.2015.53.2.337.
Praveen, G.N. and Reddy, J.N. (1998), "Nonlinear transient thermoelastic analysis of func-tionally graded ceramic-metal plates", *Int. J. Solid. Struct.*, **35**, 4457-4471. https://doi.org/10.1016/S0020-7683(97)00253-9.
Radford, D.D., Fleck, N.A. and Deshpande, V.S. (2006), "The response of clamped sandwich beams subjected to shock loading", *Int. J. Impact Eng.*, **32**(6), 968-987. https://doi.org/10.1016/j.ijimpeng.2004.08.007.
Rajabi, J. and Mohammadimehr, M. (2019), "Bending analysis of a micro sandwich skew plate using extended Kantorovich method based on Eshelby-Mori-Tanaka approach", *Comput. Concrete*, **23**(5), 361-376. https://doi.org/10.12989/cac.2019.23.5.361.
Ramteke, P.M., Panda, S.K. and Sharma, N. (2019), "Effect of grading pattern and porosity on the eigen characteristics of porous functionally graded structure", *Steel Compos. Struct*., **33**(6), 865-875. https://doi.org/10.12989/scs.2019.33.6.865.
Reddy, J.N. (1984), "A simple higher-order theory for laminated composite plates", *J. Appl. Mech.*, **51**, 745-752. https://doi.org/10.1115/1.3167719.
Reddy, J.N., Wang, C.M., Lim, G.T. and Ng, K.H. (2001), "Bending solutions of Levinson beams and plates in terms of the classical theories", *Int. J. Solid. Struct*., **38**(26-27), 4701-4720. https://doi.org/10.1016/S0020-7683(00)00298-5.
Safa, A., Hadji, L., Bourada, M. and Zouatnia, N. (2019), "Thermal vibration analysis of FGM beams using an efficient shear deformation beam theory", *Earthq. Struct*., **17**(3), 329-336. https://doi.org/10.12989/eas.2019.17.3.329.
Sahouane, A., Hadji, L. and Bourada, M. (2019), "Numerical analysis for free vibration of functionally graded beams using an original HSDBT", *Earthq. Struct*., **17**(1), 31-37. https://doi.org/10.12989/eas.2019.17.1.031.
Sedighi, H.M. and Shirazi, K.H. (2012), "A new approach to analytical solution of cantilever beam vibration with nonlinear boundary condition", *J. Comput. Nonlin. Dyn*., **7**(3), 034502. https://doi.org/10.1115/1.4005924.
Sedighi, H.M. and Shirazi, K.H. (2013), "Vibrations of micro-beams actuated by an electric field via Parameter Expansion Method", *Acta Astronautica*, **85**, 19-24. https://doi.org/10.1016/j.actaastro.2012.11.014.
Sedighi, H.M., Keivani, M. and Abadyan, M. (2015), "Modified continuum model for stability analysis of asymmetric FGM double-sided NEMS: Corrections due to finite conductivity, surface energy and nonlocal effect", *Compos. Part B: Eng.*, **83**, 117-133. https://doi.org/10.1016/j.compositesb.2015.08.029.
Sedighi, H.M., Shirazi, K.H. and Attarzadeh, M.A. (2013), "A study on the quintic nonlinear beam vibrations using asymptotic approximate approaches", *Acta Astronautica*, **91**, 245-250. https://doi.org/10.1016/j.actaastro.2013.06.018.
Sedighi, H.M., Shirazi, K.H. and Zare, J. (2012a), "Novel equivalent function for deadzone nonlinearity: applied to analytical solution of beam vibration using He's Parameter Expanding Method", *Lat. Am. J. Solid. Struct.,* **9**(4), 443-452. https://doi.org/10.1590/s1679-78252012000400002.
Sedighi, H.M., Shirazi, K.H., Reza, A. and Zare, J. (2012b), "Accurate modeling of preload discontinuity in the analytical approach of the nonlinear free vibration of beams", *Proc. Inst. Mech. Eng., Part C: J. Mech. Eng. Sci*., **226**(10), 2474-2484. https://doi.org/10.1177/0954406211435196.
Selmi, A. and Bisharat, A. (2018), "Free vibration of functionally graded SWNT reinforced aluminum alloy beam", *J. Vibroeng.*, **20**(5), 2151-2164. https://doi.org/10.21595/jve.2018.19445.
Shahadat, M.R.B., Alam, M.F., Mandal, M.N.A. and Ali, M.M. (2018), "Thermal transportation behaviour prediction of defective graphene sheet at various temperature: A Molecular Dynamics Study", *Am. J. Nanomater.*, **6**(1), 34-40. https://doi.org/10.12691/ajn-6-1-4.
Sharma, J.N., Chand, R. and Othman, M.I.A. (2009), "On the propagation of Lamb waves in viscothermoelastic plates under fluid loadings", *Int. J. Eng. Sci*., **47**(3), 391-404. https://doi.org/10.1016/j.ijengsci.2008.10.008.
Shi, G. (2007), "A new simple third-order shear deformation theory of plates", *Int. J. Solid. Struct.*, **44**, 4399-4417. https://doi.org/10.1016/j.ijsolstr.2006.11.031.
Sobhy, M. (2013), "Buckling and free vibration of exponentially graded sandwich plates resting on elastic foundations under various boundary conditions", *Compos. Struct*., **99**, 76-87. https://doi.org/10.1016/j.compstruct.2012.11.018.
Thai, C.H., Ferreira, A., Bordas, S., Rabczuk, T. and Nguyen-Xuan, H. (2014), "Isogeometric analysis of laminated composite and sandwich plates using a new inverse trigonometric shear deformation theory", *Eur. J. Mech.-A/Solid.*, **43**, 89-108. https://doi.org/10.1016/j.euromechsol.2013.09.001.
Touratier, M. (1991), "An efficient standard plate theory", *Int. J. Eng. Sci.*, **29**, 901-916. https://doi.org/10.1016/0020-7225(91)90165-Y.
Woo, J., Meguid, S.A. and Ong, L.S. (2006), "Nonlinear free vibration behavior of functionally graded plates", *J. Sound Vib.*, **289**, 595-611. https://doi.org/10.1016/j.jsv.2005.02.031.
Yazdani, R. and Mohammadimehr, M. (2019), "Double bonded Cooper-Naghdi micro sandwich cylindrical shells with porous core and CNTRC face sheets: Wave propagation solution", *Comput. Concrete*, **24**(6), 499-511. https://doi.org/10.12989/cac.2019.24.6.499.
Yüksela, Y.Z. and Akbaş, S.D. (2018), "Free vibration analysis of a Cross-Ply laminated plate in thermal environment", *Int. J. Eng. Appl. Sci. (IJEAS)*., **10**(3), 176-189. http://dx.doi.org/10.24107/ijeas.456755.
Yüksela, Y.Z. and Akbaş, S.D. (2019), "Buckling analysis of a fiber reinforced laminated composite plate with porosity", *J. Comput. Appl. Mech*., **50**(2), 375-380. https://doi.org/10.22059/jcamech.2019.291967.448.
Zenkour, A.M. and Radwan, A.F. (2018), "Compressive study of functionally graded plates resting on Winkler-Pasternak foundations under various boundary conditions using hyperbolic shear deformation theory", *Arch. Civil Mech. Eng.*, **18**, 645-658. https://doi.org/10.1016/j.acme.2017.10.003.
Zhang, D.G. and Zhou, Y.H. (2008), "A theoretical analysis of FGM thin plates based on physical neutral surface", *Comput. Mater. Sci.*, **44**, 716-720. https://doi.org/10.1016/j.commatsci.2008.05.016.
Zhou, Y., Wang, Q., Shi, D., Liang, Q. and Zhang, Z. (2017), "Exact solutions for the free in-plane vibrations of rectangular plates with arbitrary boundary conditions", *Int. J. Mech. Sci*., **130**, 1-10. https://doi.org/10.1016/j.ijmecsci.2017.06.004.
Zouatnia, N. and Hadji, L. (2019), "Effect of the micromechanical models on the bending of FGM beam using a new hyperbolic shear deformation theory", *Earthq. Struct.*, **16**(2), 177-183. https://doi.org/10.12989/eas.2019.16.2.177.

CC